

Real-Time Time-Dependent Density Functional Theory for Simulating Nonequilibrium Electron Dynamics

Jianhang Xu, Thomas E. Carney, Ruiyi Zhou, Christopher Shepard, and Yosuke Kanai*



Cite This: *J. Am. Chem. Soc.* 2024, 146, 5011–5029



Read Online

ACCESS |

Metrics & More

Article Recommendations

Downloaded via NORTHWESTERN UNIV on July 18, 2025 at 03:52:44 (UTC).
See https://pubs.acs.org/sharingguidelines for options on how to legitimately share published articles.

ABSTRACT: The explicit real-time propagation approach for time-dependent density functional theory (RT-TDDFT) has increasingly become a popular first-principles computational method for modeling various time-dependent electronic properties of complex chemical systems. In this Perspective, we provide a nontechnical discussion of how this first-principles simulation approach has been used to gain novel physical insights into nonequilibrium electron dynamics phenomena in recent years. Following a concise overview of the RT-TDDFT methodology from a practical standpoint, we discuss our recent studies on the electronic stopping of DNA in water and the Floquet topological phase as examples. Our discussion focuses on how RT-TDDFT simulations played a unique role in deriving new scientific understandings. We then discuss existing challenges and some new advances at the frontier of RT-TDDFT method development for studying increasingly complex dynamic phenomena and systems.

1. INTRODUCTION

Most electronic structure theory problems entail approximately solving the time-independent Schrödinger equation for a Fermionic system specified by a given Hamiltonian. At the same time, various physical properties derive from the response of the Fermionic system of electrons to an external time-dependent perturbation. In situations where the external perturbation is slowly varying, we are in the adiabatic limit such that the electrons remain in the equilibrium ground state and the response can be studied by solving for the instantaneous eigenstate of the time-dependent Hamiltonian. The reciprocal interplay between atomic nuclear dynamics and electrons, as necessary for studying properties at finite temperatures, can be treated in this manner in most cases, and first-principles molecular dynamics (FPMD) based on density functional theory (DFT)¹¹ has found great success in various areas of chemistry and condensed matter physics.¹² The appealing balance between accuracy and efficiency, together with its formal theoretical foundation based on the Hohenberg–Kohn theorem, has made DFT calculations particularly popular, especially for situations when complex systems need to be studied under various conditions of temperatures and pressures. However, when the external perturbation is fast-varying, the time evolution of the quantum state needs to be explicitly described by solving the time-dependent Schrödinger equation instead of assuming that the electrons remain in the ground state. The quantum-mechanical response of electrons to light, as described by the time-dependent electromagnetic field, is an example of such a situation. External stimuli like the electromagnetic field introduce additional vector and/or scalar potentials in the system's Hamiltonian, and dynamical response to such time-dependent perturbation is encoded in the time evolution of the quantum state. Although optically induced electronic excitation is inherently a time-dependent quantum-mechanical

phenomenon, a great deal about such a process like resonating transition energies can be learned by staying within the linear response theory formalism. Indeed, time-dependent density functional theory (TDDFT)^{13,14} is widely used for calculating the excitation energies with the linear response approximation without explicitly modeling the quantum dynamics of electrons in response to the electromagnetic field.^{15–19} At the same time, the theoretical formalism of TDDFT is based on the Runge–Gross theorem,¹³ and it offers a powerful extension to DFT for studying dynamical phenomena^{14,20–23} in general beyond the linear response theory approach.^{15–17}

Starting with the time-dependent Hartree–Fock theory in the late 70s and early 80s,²⁴ various theoretical methodologies, including those based on correlated wave function methods,²⁵ have been developed for studying nonequilibrium response properties by explicitly solving the time-dependent Schrödinger equation in the parameter-free framework of first-principles theory. In these approaches, the quantum dynamics of electrons are simulated numerically, and nonequilibrium properties are obtained from “trajectories” in quantum dynamics. Among the first-principles electronic structure methods developed for this explicit real-time propagation, TDDFT is particularly suitable for studying complex extended systems. Today, it is probably one of the few, if not the only, practical computational methods for investigating nonequilibrium electron dynamics in condensed phase systems. Readers are referred to the comprehensive review by Li et al. on the

Received: July 31, 2023

Revised: January 23, 2024

Accepted: January 23, 2024

Published: February 16, 2024



development of the real-time propagation approaches for electronic structure theory methods in general.²⁶ In the last few decades, the real-time propagation approach for TDDFT (RT-TDDFT)²⁷ has garnered great attention as a particularly practical methodology for studying the nonequilibrium response of complex systems including extended condensed phase matters because of its appealing balance between accuracy and efficiency. The real-time propagation approach allows us to expand the scope of the investigation beyond the linear response or the traditional perturbative regimes with TDDFT, and RT-TDDFT simulations are increasingly employed to help answer various outstanding questions, especially of nonequilibrium electron dynamical phenomena. While its first use can be found as early as in the late 80s and early 90s,^{27,28} the RT-TDDFT approach became rather popular only in the past decade. This is partly due to the growing availability of powerful high-performance computers, since RT-TDDFT simulations are computationally much more demanding than the ground-state DFT calculations. This Perspective will focus on how recent advances in the RT-TDDFT method enable us to gain new scientific insights from first-principles theory by discussing a few examples from our own work. Although the mathematical/numerical aspects of RT-TDDFT simulation are essential for method developers in the community, we refrain from such technical discussion in this Perspective.

2. REAL-TIME PROPAGATION APPROACH FOR TDDFT

Since Theilhaber²⁹ and Yabana and Bertsch^{27,28} reported some of the first uses of the real-time propagation approach with TDDFT, the RT-TDDFT simulation has gained great popularity in various areas of chemistry and condensed-matter physics.^{30–36} In addition to its utility in calculating optical absorption spectra,^{28,30,37–39} especially when the linear response approach faces difficulty,⁴⁰ RT-TDDFT has become a valuable method for studying a wide range of excited-state phenomena such as interfacial charge transfer,^{41,42} electronic stopping,^{43–52} core electron excitations,^{4,53–56} electronic circular dichroism spectra,⁵⁷ exciton dynamics in nanostructures,^{58,59} atom-cluster collisions,^{60,61} high harmonic generation,^{62,63} laser-induced water splitting,⁶⁴ topological quantum matter,^{2,5,65,66} etc. The RT-TDDFT method has been implemented nowadays in a variety of electronic structure codes, including NWChem,^{30,67} SIESTA,^{54,68,69} CP2K,^{70,71} SALMON,⁷² Octopus,^{73,74} Q-Chem,^{75–77} GAUSSIAN,^{34,78} MOLGW,^{79,80} Qbox/Qb@ll,^{81–83} FHI-aims,⁸⁴ etc. Numerical implementations vary greatly among these computer codes, especially in the underlying basis sets used, and the periodic boundary conditions have been adapted for investigating extended systems in some of these codes. While we do not discuss the technical aspects of RT-TDDFT in this Perspective, we note that the numerical implementation details are relevant also for users of these computer codes because the most appropriate and convenient implementation of the theory is often dictated by the type of phenomena investigated. For instance, plane-wave pseudopotential (PW-PP) formulation^{83,85} is highly suitable when the ionization is dominant in the excitation phenomenon investigated because the basis set functions are highly extended and not centered on atomic nuclei. At the same time, the PW-PP formulation may not be the most convenient framework for investigating core-electron excitation because it would require very large numbers

of plane-waves for achieving convergence along with great care in generating accompanying pseudopotentials.⁴ All-electron formulations such as those based on a numeric atom-centered orbital (NAO) approach⁸⁴ are likely more suitable in such situations.⁸⁴

Before discussing how RT-TDDFT simulation is used for obtaining new scientific understanding, we briefly outline the underlying theory without dwelling on methodological details, which are important but discussed elsewhere in the literature.¹⁴ TDDFT is based on the one-to-one correspondence between the time-dependent one-particle probability density and the time-dependent external potential. This correspondence is formally established by the Runge-Gross theorem,¹³ which extends the Hohenberg-Kohn theorem to time-dependent cases. There are several notable assumptions in the proof, such as the Taylor-expandable potential, and we refer to the textbook by Ullrich for a thorough discussion of these aspects of TDDFT as a formal theory in quantum mechanics.¹⁴ While many problems in electronic structure theory can be cast as some form of an eigenvalue problem, RT-TDDFT instead entails solving a set of coupled nonlinear differential equations. At the heart of RT-TDDFT simulation, there is the time-dependent Kohn-Sham (TD-KS) equation

$$i\frac{\partial}{\partial t}\phi_n(\mathbf{r}, t) = \left\{ \frac{1}{2}(-i\nabla + \mathbf{A}(\mathbf{r}, t) + \mathbf{A}_{\text{XC}}(\mathbf{r}, t))^2 + \hat{\nu}_{\text{ext}}(\mathbf{r}, t) + \int d\mathbf{r}' \frac{\rho(\mathbf{r}', t)}{|\mathbf{r} - \mathbf{r}'|} + \hat{\nu}_{\text{XC}}(\mathbf{r}, t) \right\} \phi_n(\mathbf{r}, t) \quad (1)$$

where $\phi_n(\mathbf{r}, t)$ is the n -th TD-KS single-particle orbital and $\rho(\mathbf{r}, t)$ is the electron density. The Brillouin zone integration is often important for modeling extended systems, and then, the index n needs to be understood as a composite index that consists of both the momentum wavevector in the first Brillouin zone and the state index; the TD-KS orbitals would then obey Bloch's theorem such that $\phi_{s,k}(\mathbf{r}, t) = e^{i\mathbf{k}\cdot\mathbf{r}}u_{s,k}(\mathbf{r}, t)$ in which $u_{s,k}(\mathbf{r}, t)$ is the lattice periodic part. $\mathbf{A}(\mathbf{r}, t)$ and $\hat{\nu}_{\text{ext}}(\mathbf{r}, t)$ terms account for all external potentials acting on electrons, including those due to atom nuclei and applied external electric and magnetic fields. $\hat{\nu}_{\text{XC}}$ is the exchange-correlation (XC) potential, which is approximated in practice, as discussed later. While the XC vector potential, $\mathbf{A}_{\text{XC}}(\mathbf{r}, t)$, is typically absent in most XC approximations, this term becomes highly relevant for describing exciton dynamics using the RT-current-TDDFT formulation,¹⁴ as briefly discussed in a later section. This TD-KS differential equation looks as if it were a time-dependent Schrödinger equation. However, a particular numerical complexity arises because the electron density is given by the TD-KS orbitals as $\rho(\mathbf{r}, t) = \sum_n^{\text{Occ.}} |\phi_n(\mathbf{r}, t)|^2$. The Kohn-Sham Hamiltonian (the curly bracket in eq 1) depends on the electron density (thus, on the TD-KS orbitals), and this dependence makes TD-KS differential equations nonlinear. The nonlinearity makes the numerical integration of the TD-KS orbitals particularly susceptible to the instability,⁸⁵ and this nonlinear feature also makes it difficult to apply some analytical approaches developed for model Hamiltonians. For instance, for Hamiltonians with a periodically driven potential, it is usually straightforward to obtain a stationary solution via the construction of an effective Hamiltonian within the framework of the Floquet theory. However, the KS Hamiltonian's dependence on the TD-KS orbitals complicates applying such well-established analytical formalisms.

For the numerical propagation, the time evolution of the TD-KS orbitals can be expressed in the integral form as

$$\{|\phi_n(t)\rangle = \hat{U}(t, t_0)|\phi_n(t_0)\rangle\}_{n=1...Occ.} \quad (2)$$

where the propagation operator is given by

$$\begin{aligned} \hat{U}(t, t_0) = \hat{1} + \sum_{k=0} \frac{1}{k!} \left(-\frac{i}{\hbar} \right)^k \int_{t_0}^t dt_1 \int_{t_0}^{t_1} dt_2 \dots \\ \int_{t_0}^t dt_k \hat{\mathcal{T}}[\hat{H}_{KS}(t_1)\hat{H}_{KS}(t_2)\dots\hat{H}_{KS}(t_k)] \end{aligned} \quad (3)$$

where $\hat{\mathcal{T}}$ is the time-ordering operator and \hat{H}_{KS} is the KS Hamiltonian. Note that the Hamiltonians at different times do not commute in general, and the propagation operator (eq 3) needs to be approximated with a sequence of many but a finite number of propagation steps with a small dt , making numerical integration essential for the real-time propagation approach. In practice, one needs to ensure that dt is small enough for performing an accurate integration in time. Simply put, RT-TDDFT simulation amounts to numerically integrating the TD-KS orbitals in time according to the TD-KS equation (eq 1) for a given initial state $\{\phi_n(\mathbf{r}, t=0)\}_{n=1...Occ.}$. Numerical methods for solving nonlinear differential equations like the TD-KS equation continue to remain a very active area of computational mathematics research with great impacts on various fields including RT-TDDFT simulation, and a more detailed discussion of this aspect is found elsewhere.^{85–87}

Importantly, the time-dependent electron density, $\rho(\mathbf{r}, t)$, remains invariant with respect to different sets of TD-KS orbitals that one can obtain through a unitary transformation of the time-dependent orbitals. This gauge freedom (choice) is inconsequential to physical observables which are formally dependent on the density. This gauge invariance yields certain constraints on the XC potential form in the context of TDDFT as a formal theory. In practical simulations, this gauge freedom has been exploited for numerical convenience^{88,89} as well as for deriving conceptual understandings from RT-TDDFT simulation.^{3,90} For instance, Lin and co-workers have developed so-called parallel transport gauge in which an optimal gauge is found to minimize oscillations of individual TD-KS orbitals.⁸⁸ This allows for a much larger integration time step to be used than normally possible. The concept of the natural transition orbitals⁹¹ has been also extended to the RT-TDDFT approach using this gauge freedom such that nonequilibrium dynamics can be optimally represented in the particle-hole excitation picture.⁹⁰ For developing a molecular-level understanding, the so-called maximally localized Wannier functions (MLWFs) have proved particularly useful.⁹² For isolated molecular systems, the Boys orbitals that minimize the spatial extent of individual orbitals have been widely used for deriving insights into the nature of chemical bonds. MLWFs are generalizations of the Boys orbitals for extended systems with the Brillouin zone, and they constitute a set of maximally localized orbitals that are constructed through unitary transformation of the single-particle KS orbitals. The underlying electron dynamics remain invariant even when the MLWFs are propagated in RT-TDDFT simulation since $\rho(\mathbf{r}, t) = \sum_i^{\text{Occ.}} |w_i(\mathbf{r}, t)|^2$ ²² and the quantum dynamics of electrons are governed by the time-dependent electron density $\rho(\mathbf{r}, t)$ according to the Runge-Gross theorem.¹³ Figure 1 depicts how MLWFs are obtained through the unitary transformation for the H₂ chain and crystalline silicon as examples. In condensed phase systems,

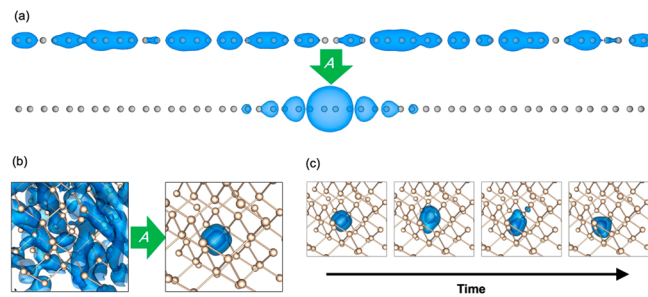


Figure 1. A representative delocalized Bloch state and a maximally localized Wannier function (MLWF) resulting from the unitary transformation for (a) an infinite H₂ chain and (b) the crystalline silicon. (c) Time evolution of the MLWF in the crystalline silicon in the RT-TDDFT simulation. Adapted with permission from ref 2. Copyright 2019 AIP Publishing.

TD-KS orbitals are usually highly delocalized, as shown in Figure 1a,b. Application of the suitable unitary operator, as denoted by “A”, allows one to maximally localize the set of the valence (occupied) TD-KS orbitals without changing physically observable time-dependent properties. Performing RT-TDDFT simulation by propagating the MLWFs has proved particularly useful,⁹² and we extensively refer to this concept in this Perspective.

3. NOVEL INSIGHTS FROM RT-TDDFT SIMULATION

Owing to its nonperturbative description of quantum dynamics, RT-TDDFT methodology has been used extensively for studying nonlinear effects in photoexcitation such as the Landau-like damping of plasmon excitation^{58,93–95} and photo-induced charge transfer at heterojunctions.^{41,96} RT-TDDFT can also provide physical insights into other types of dynamical phenomena by explicitly simulating nonequilibrium electron dynamics with atomistic details. We focus on this relatively underexplored aspect by illustrating how this first-principles approach has helped advance a few important fields by contributing to new understanding at the molecular level. As examples from our recent work, we discuss here the electronic stopping of DNA in water and the emergence of the Floquet topological phase in molecular systems. The DNA electronic stopping is an exemplifying case of how first-principles theory contributes to advancing a century-old field of study,⁴⁴ and new molecular-level understanding can be developed for the promising medical technology of ion beam cancer therapy at the same time. We discuss the study of the Floquet topological phase as another example to showcase how the first-principles simulation of nonequilibrium electron dynamics helps advance the emerging field of fundamental scientific interest and excitement, while the field has progressed mostly within the model Hamiltonian framework.

3.1. Electronic Stopping of DNA. When the energy/momentum transfer from a fast-moving charged particle to electrons is responsible for slowing down the projectile particle in matter, this dynamical process is generally termed electronic stopping. Stopping power, as a property of a particular matter to decelerate the penetrating high-energy charged particle, has been studied for more than a century since Rutherford's first experiment with α -particles.^{44,97} At low velocities, the charged particle loses its kinetic energy to the lattice ions in the target matter, while the electrons largely remain in the ground state in this so-called nuclear stopping regime. When the velocity is much higher, the charged particle loses its kinetic energy to

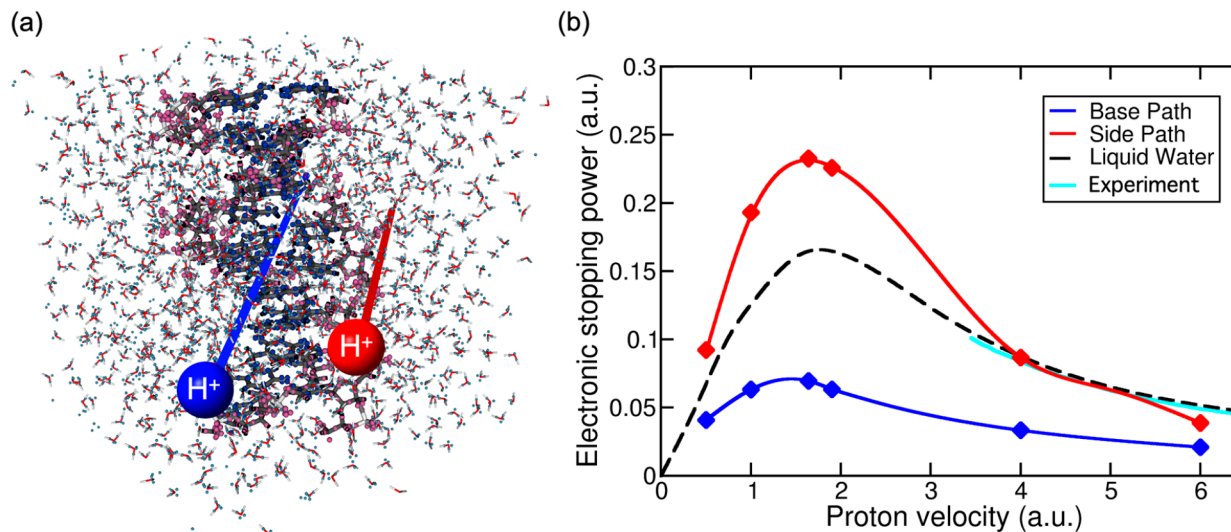


Figure 2. (a) Solvated DNA structure in water, with the equilibrium MLWF centers shown as light blue spheres (on water), dark blue spheres (on nucleobases), and magenta spheres (on sugar–phosphate side chains). The Base path for the projectile proton is denoted by the blue line, and the Side path is denoted by the red line. (b) Electronic stopping power of DNA in water for the proton with the Base and Side paths. Electronic stopping power of liquid water is shown with a black dashed line as the reference.⁴ The experimental electronic stopping power of liquid water by Shimizu and co-workers is shown in cyan for comparison.^{6,7} Adapted with permission from ref 10. Copyright 2023 the American Physical Society.

electrons via electronic excitations due to Coulomb interaction. From the viewpoint of electronic structure theory, electronic stopping is particularly interesting because the chemical bonding environment has a significant effect on the stopping power.⁴⁷ The quantum-mechanical energy-transfer dynamics responsible for electronic stopping is a highly out-of-equilibrium process, and its rate depends strongly on the velocity of the charged particle. Electronic stopping power is the rate at which the kinetic energy (momentum) of the charged particle is transferred to matter via electronic excitation. This velocity-dependent function is generally given per unit distance of the traveling particle, and great efforts have been devoted to the calculation of this property over the last century. Along with the seminal Bethe formula from 1930,⁹⁸ Lindhard's linear response theory based on the dielectric function⁹⁹ in 1954 marks a major milestone in the long history of electronic stopping power calculation. A few informative reviews on this topic are available elsewhere.^{100,101}

In more recent years, parameter-free first-principles calculations have been used to calculate the dielectric function of real matter within the framework of linear response theory.¹⁰² In the past decade or so, an accurate determination of the electronic stopping power has become possible using RT-TDDFT nonequilibrium simulation,^{44,45,101} and this first-principles theory approach has been successfully applied to various matters, including metallic and semiconductor solids, liquids, and DNA.^{4,44,45,47–50,103–105} In addition to accurate calculation of this important property, the RT-TDDFT simulation also provides molecular-level details of the electronic excitations induced by the charged particle as it transfers its kinetic energy to electrons in the target matter. Such molecular-level understanding of the electronic excitation is particularly important for studying the electronic stopping process of highly heterogeneous systems like DNA in water.¹⁰

The electronic stopping process of high-energy protons in DNA/water has garnered significant interest in recent years because of its central role in proton beam cancer therapy, emerging as a highly promising radiation oncology treat-

ment.^{4,10,51,106} The electronic stopping power for high-energy protons (with the initial kinetic energy of a few hundred keV or higher) in liquid water is used as the baseline for calibrating the proton beam by developing an energy deposition profile for human tissue together with the computed tomography scan.¹⁰⁷ At the same time, DNAs in tumor cells are the physical target in which damaging electronic excitation is induced as a result of the electronic stopping process via the “direct” effect, which is believed to be the dominant mechanism for ion beam therapies.¹⁰⁸ In addition to providing an accurate electronic stopping power for liquid water, which is a very difficult property to obtain experimentally due to the use of particle accelerators,^{6,7} RT-TDDFT can be used to directly simulate how high-energy protons transfer the kinetic energy to DNA via electronic excitation. Formulating it as the nonadiabatic retarding force,^{46,101} the electronic stopping power can be calculated from the electronic energy change as the projectile particle travels at a constant velocity, v , in a nonequilibrium simulation.⁴⁷ In such simulations, the constant of motion is not the energy by itself but the energy and the work done on the system by the projectile ion. Then, the electronic stopping power can be obtained as $S_e(v) = \langle \dot{E}[\rho(t)] \rangle_{v,v}^{-1}$.^{44,101} The angle bracket here denotes the classical ensemble average as the projectile particle travels through the target matter at a constant velocity v , and \dot{E} here represents the time derivative of the total electronic energy. This velocity-dependent function, the stopping power, is obtained by performing a series of RT-TDDFT simulations with various values for the projectile particle velocity, v . This RT-TDDFT approach was successfully used to calculate an accurate parameter-free electronic stopping power of liquid water including the crucial part of the stopping power curve near the peak,⁴ which was not accessible in the experiments by Shimizu and co-workers.^{6,7} Excellent agreement of the RT-TDDFT electronic stopping power curve with the available experimental data is seen in Figure 2b while various linear response theory models including the Bethe theory⁹⁸ deviate considerably from the

RT-TDDFT simulation result and from the experimental data as discussed in ref 4.

The electronic stopping power curve for liquid water is central to developing the energy deposition profile for patients in ion beam radiation therapy.¹⁰⁹ At the same time, the fundamental scientific question of how the kinetic energy is transferred from the high-energy protons to the DNA remains despite its importance for developing a mechanistic understanding of DNA damage.^{110–112} Many studies indicate that the proton beams yield complex clustering lesions with strand breaks, including double-strand breaks, as the direct effect of high-energy proton irradiation on DNA.¹¹³ These strand lesions, particularly with other lesions nearby, are much more likely to lead to cell death.¹¹⁴ The direct effect appears relatively more important for ion radiation than for photon-based radiation when compared to the indirect effect in which DNA damage is indirectly caused by byproducts of radiation-induced excitation/ionization of water molecules.¹⁰⁸ Currently, how the proton beam induces DNA lesions is not understood at the molecular level,¹¹⁵ and details of the energy-transfer mechanism from irradiating high-energy protons to DNA are needed to help fill this crucial knowledge gap.¹¹⁶

RT-TDDFT simulation can be used to examine how electronic excitations are induced in different molecular motifs of DNA as a high-energy proton penetrates through the DNA in water as shown in Figure 2.¹⁰ The simulated system of DNA solvated in water contains more than 11,000 electrons, and Figure 2a shows the position expectation values of all the MLWFs at equilibrium, together with the two projectile proton paths studied. The calculated electronic stopping power is shown for these Side and Base paths in Figure 2b. Counterintuitively, a much greater stopping power (i.e., the energy-transfer rate) is observed for the Side path, and the stopping power for the Side path is much higher than that of water, particularly near the peak of the stopping power curve. High-energy protons would irradiate uniformly in space on the scale of individual DNAs in a proton beam, and thus, an important question is which parts of DNA are electronically excited by the high-energy protons. The use of the Wannier gauge is very helpful here, as we can examine the extent to which individual time-dependent MLWFs, which are spatially localized on different DNA moieties, dynamically respond to the projectile proton. The RT-TDDFT simulation shows that significant electronic excitations take place on the sugar-phosphate side chains rather than on the nucleobases of DNA for the Side path, which exhibits a particularly large electronic stopping power.¹⁰ Interestingly, the significant excitations induced on the phosphate side chains are due to the lone-pair electrons, which, in water, are exposed on the deprotonated phosphate groups. These electrons tend to be highly polarizable, but the perturbing electric field from the projectile proton is confined close to the proton path. Therefore, these lone-pair electrons are effectively excited only by the projectile protons that come close to them around the sugar–phosphate side chains. Because of the localized nature of the electric field from the projectile proton, the Base path does not show significant excitation on the DNA side chains as discussed in detail in ref 10. These RT-TDDFT simulations address only the initial excitation stage. To develop a complete picture of DNA damage with ion irradiation, dynamics on longer times also need to be studied as they involve relaxation of the charge carriers^{117,118} and chemical reaction dynamics.¹⁰

First-principles approaches like RT-TDDFT also provide a convenient means to study how atomistic changes impact nonequilibrium electron dynamics, especially when experiments are challenging and costly. The proton beam has been increasingly used in radiation oncology^{116,119} in spite of the high cost of constructing and operating cyclotrons for accelerating protons,^{120–123} and some have even advocated for the use of heavier ions. This is because a larger energy transfer can be expected for higher-Z ions according to linear response theory.^{120,124–128} However, for higher-Z ions, such as α -particles and carbon ions, our understanding of the electronic stopping process is even more tenuous. In addition to having various contradicting experimental measurements,^{129–131} widely used models based on the linear response theory fail to predict the electronic stopping power change with the projectile ion type.⁴⁹ The RT-TDDFT approach enables us to move beyond such a linear response theory description, allowing us to examine how the electronic stopping power changes with α -particles and carbon ions as the irradiating high-energy particles.¹³² Figure 3 shows the

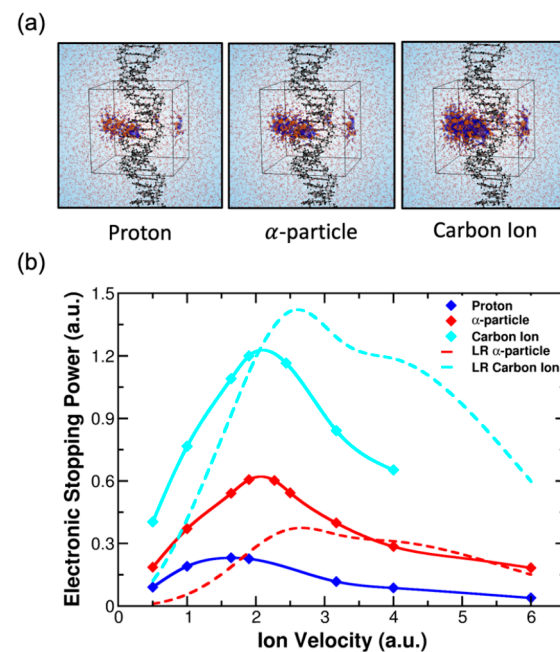


Figure 3. (a) Electron density changes (with respect to the equilibrium ground state) for different irradiating ion types of proton, α -particle, and carbon ion as the projectile particle in the Side path at the stopping power peak velocities. The simulation supercell with the periodic boundary conditions is outlined by the black line. Blue (orange) isosurfaces represent increases (decreases) in the electron density in response to the projectile ion. (b) Electronic stopping power of DNA in water for the different irradiating ion types for the Side path. The stopping powers for α -particle and carbon ion, obtained by applying the linear response (LR) theory to the proton's stopping power, are also shown as the dashed lines. For the LR models, the velocity dependence of the projectile ion charge was accounted for by calculating the values from RT-TDDFT simulation.

stopping power for the Side path as a function of the ion velocity for protons, α -particles, and carbon ions. The stopping power changes considerably but not as predicted by the linear response theory, according to which the stopping power scales quadratically with the ion charge and the stopping power peak position depends only on the target matter (i.e., DNA/water).

Even when the velocity dependence of the ion's charge is taken into account, the linear response theory results deviate considerably from the RT-TDDFT simulation results for the α -particle and carbon ion as seen in Figure 3b. For both α -particles and carbon ions, the linear response theory underestimates the stopping power by as much as 40% at velocities close to the stopping power peak while also failing to predict the correct peak velocity. RT-TDDFT offers a direct nonperturbative approach to examining how the electronic stopping dynamics change for complex heterogeneous systems with different high-energy ions beyond the usual linear response theory.¹³³

Although we do not wish to dwell on the computational details of RT-TDDFT simulation in this Perspective, let us discuss a few practical considerations. These simulations of DNA in the water represent some of the largest first-principles quantum dynamics simulations with more than 11,000 electrons. In terms of the basis set functions, more than six million plane-waves were necessary to converge the calculation. In practical calculations, the accuracy of such simulation depends not only on the underlying theory and related approximations such as the XC approximation (so-called generalized gradient approximation (GGA)¹³⁴ was used here) but also on the computational setups like the convergence of the simulation box size for complex extended systems and the basis set functions, etc. In order to converge the calculations with respect to these computational settings/parameters, the capability to perform large-scale simulations on modern massively parallel high-performance computers (HPCs) is essential. Therefore, tremendous efforts are spent on the numerical implementation of RT-TDDFT methodology as a code/software^{83,135,136} such that simulations can take advantage of modern HPCs with hundreds of thousands of processors. For the RT-TDDFT simulation of DNA in water, more than 250,000 processors of Theta HPC at Argonne National Laboratory are used for the computation. The software needs to evolve also in response to the changing landscape of HPCs such as those represented by the emergence of GPU-based machines,¹³⁷ and this aspect tends to be underappreciated in many fields despite its practical importance.

This particular example showcased how RT-TDDFT simulations can help answer some of the most outstanding scientific questions of great societal importance using modern HPCs, especially notable since experiments are difficult to perform (e.g., due to the necessary use of particle accelerators). At the same time, there are still various challenges in the theoretical aspect. In particular, the adequacy of the XC approximation is one of the most important considerations in any DFT-based calculations, including RT-TDDFT simulation. Whenever possible, it is important to assess its accuracy by performing certain aspects of simulation using a higher-level XC approximation as we have done, for example, for liquid water in ref 4. With advanced XC approximations, however, the computational cost tends to increase rather dramatically, especially with some of the advanced XC approximations based on so-called hybrid functionals. New algorithmic innovations continue to play an important role in advancing our ability to perform more accurate calculations on increasingly complex systems like solvated DNA in water, and this aspect is discussed in the following section (Section 4).

3.2. Floquet Topological Phase. The second example here illustrates how RT-TDDFT can advance our fundamental

understanding, in this case, of how certain physical properties are determined by the topological character of the time-dependent Hamiltonian. We focus on a particular work that connects the mathematical formulation of nonadiabatic Thouless pumping to a chemically intuitive description on the molecular level.^{5,138} One of the earliest realizations that topological characteristics of the Hamiltonian govern certain dynamical properties came from Thouless in 1983 when the quantized pumping phenomenon was predicted.¹³⁹ This seminal work on quantized particle transport in a one-dimensional system showed that the quantization derives from the topology of the underlying quantum-mechanical Hamiltonian. Under the adiabatic (i.e., instantaneous eigenstates) and time-periodic evolution of the Hamiltonian, one can show that the particle current is given by a topological invariant called winding number. For topological insulators, the winding number can take a nonzero integer value while it is zero for normal/trivial insulators. The intricacy of the Hamiltonian can be recovered conveniently in the phase information on wave function (particularly important for studying real systems instead of model Hamiltonians), and it has a close connection to the modern theory of polarization developed in the 90s.^{140,141} In recent years, Thouless pumping has been demonstrated experimentally in various systems^{142,143} including an ultracold Fermi gas¹⁴⁴ and atoms in optical lattice.¹⁴⁵

An interesting recent development is the idea of so-called topological Floquet engineering; that is to use a time-periodic field to induce a topological phase in a driven system that is otherwise a trivial insulator.^{146,147} In a Floquet system, the time-dependent Hamiltonian satisfies $\hat{H}(t+T) = \hat{H}(t)$ and an effective time-independent Hamiltonian can be defined via the evolution operator over one periodic time T such that $\hat{H}_{\text{eff}}(k) \equiv iT^{-1} \ln \left\{ \hat{\mathcal{T}} \exp \left[-i \int_0^T dt \hat{H}(k, t) \right] \right\}$ where $\hat{\mathcal{T}}$ is the time-ordering operator and k is the reciprocal wavenumber of a one-dimensional system. The winding number, being equal to the integrated particle current over the periodic time T , can be given in terms of the energy spectrum of this effective Floquet Hamiltonian, ϵ_i (quasienergy), or equivalently in terms of nonadiabatic Aharonov-Anandan geometric phase¹⁴⁸ of the Floquet states. Conveniently for electronic structure theory, the winding number can be expressed in terms of time-dependent Bloch states, $u_n(k, t)$, as^{5,138}

$$W = \frac{1}{2\pi} \sum_n^{\text{occ.}} \left[\int_{BZ} dk \langle u_n(k, t=T) | i\partial_k | u_n(k, t=T) \rangle - \int_{BZ} dk \langle u_n(k, t=0) | i\partial_k | u_n(k, t=0) \rangle \right] \quad (4)$$

One may note that the winding number can be expressed analogously to the static Chern insulator, as $W = C \equiv \frac{1}{2\pi} \int_0^T dt \int_{BZ} dk \sum_n^{\text{occ.}} F_n(k, t)$ where C would be the first Chern number of the Floquet states, and the generalized Berry curvature is given by $F_n(k, t) = i[\langle \partial_t u_n(k, t) | \partial_k u_n(k, t) \rangle - \langle \partial_k u_n(k, t) | \partial_t u_n(k, t) \rangle]$.¹⁴¹ Using the Blount identity $\langle u_n(t) | \hat{p} | u_n(t) \rangle = \frac{L}{2\pi} \int_{BZ} dk \langle u_n(k, t) | i\partial_k | u_n(k, t) \rangle$, the winding number can be expressed in terms of the time-dependent MLWFs, $w_n(r, t)$, as⁵

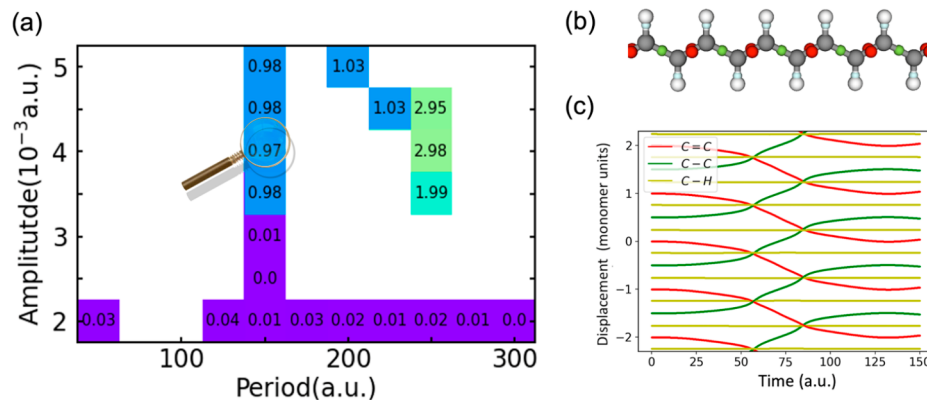


Figure 4. (a) Integrated electron current per monomer unit over one driving cycle, Q , is shown as a function of the driving electric field period (T) and amplitude ($|A|$). When the Floquet condition is satisfied, the current is an integer, given by the winding number, which is a topological property. RT-TDDFT simulation shows that the computed value is indeed an integer within some numerical accuracy. In addition to the trivial/normal insulator phase (shown in purple), Floquet topological phases with different values for the winding number are observed. See ref 5 for more details. (b) Trans-polyacetylene with MLWFs that represent $\text{C}=\text{C}$ (red), $\text{C}-\text{C}$ (green), and $\text{C}-\text{H}$ (light blue) bonds. (c) Time evolution of the Wannier centers for different MLWFs, for the $W = 1$ topological phase indicated by the magnifying glass icon in (a).

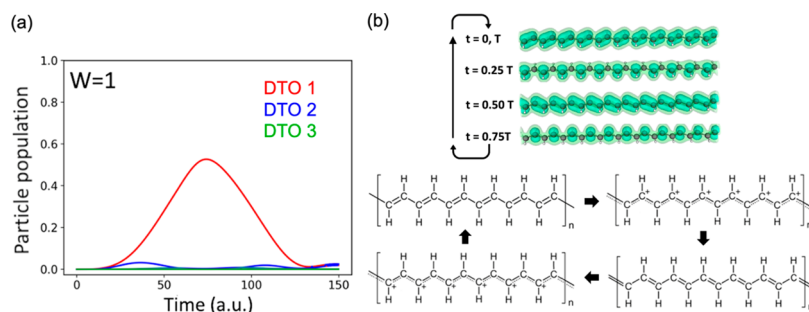


Figure 5. (a) The particle population, $p_n^2(t)$, as a function of time for the three dynamical transition orbitals (DTOs) with the most changes. A particular case of the winding number of one ($W = 1$) is shown with the driving field period, T , of 150 a.u. and the field amplitude, A , of 4×10^{-3} a.u. See Figure 4a. (b) Spatial changes of the most dominating DTO (DTO1) over one driving cycle and the corresponding chemical bond structures.

$$W = L^{-1} \sum_n^{\text{Occ.}} [\langle w_n(t=T) | \hat{w}_n(t=T) \rangle - \langle w_n(t=0) | \hat{w}_n(t=0) \rangle] \quad (5)$$

where the position operator here is defined according to the formula given by Resta for extended periodic systems¹⁴⁹ and L is the lattice length of the unit cell. The Berry phase formulation is now related to the time-dependent MLWFs, and the winding number can be interpreted intuitively as the number of the geometric centers of the Wannier functions (i.e., Wannier centers) pumped over one driving cycle, T , in the Thouless pumping.^{150,151} This formulation provides a chemically intuitive description of how the winding number physically represents the number of electrons pumped in time T , and we can connect this behavior to chemical motifs at the molecular level.¹³⁸

Using the RT-TDDFT simulation to propagate the MLWFs in time, we can calculate the winding number via eq 5, and the topological Floquet engineering was demonstrated by inducing topological phases in a trans-polyacetylene polymer.⁵ Trans-polyacetylene is an ideal molecular system since it embodies key features of the classic Su-Schrieffer-Heeger model, which is widely used to study the transition between topological insulator and normal/trivial insulator phases by artificially changing the empirical hopping parameters in the Hamiltonian between the single and double $\text{C}-\text{C}$ bonds.¹⁵² Two distinct carbon atom sites, due to the Peierls instability, give rise to the

chiral (i.e., sublattice) symmetry in the Hamiltonian. External time-periodic electric field, $E(t) = A \sin(2\pi t/T)$, is applied to the system, and we calculate the number of electrons transported, Q , in a single time period T (i.e., driving cycle) as a function of the field amplitude $|A|$ and the period T using RT-TDDFT simulation. We must note that the single-particle Kohn–Sham (KS) Hamiltonian depends on the time-dependent KS orbitals in TDDFT, and the Floquet condition (i.e., $\hat{H}(t+T) = \hat{H}(t)$) is not always satisfied even when the perturbing external potential is time-periodic. Figure 4a shows the time-integrated current, Q , as a function of the field amplitude $|A|$ and the time period T , for those combinations in which the Floquet condition is satisfied. The Floquet condition is satisfied when the determinant of the overlap matrix between the time-dependent KS orbitals at $t = 0$ and $t = T$ is unity,⁵ and Figure 4a shows the value for Q when the determinant is larger than 0.98. For these areas, the number of transported electrons, Q , is equal to the topological invariant, the winding number, W , and the RT-TDDFT simulation shows that Q is indeed quantized within the numerical precision one would expect. In the purple-colored region where $Q \approx 0$, the trivial insulator phase (i.e., $W = 0$) is observed. With a higher field amplitude, the topological phase emerges in other areas, exhibiting $W = 1, 2$, and 3 . The RT-TDDFT simulation can also yield physical insights for understanding how Floquet topological phases emerge by analyzing the quantum dynamics of electrons in terms of valence bond theory.⁵ The spatially

localized maximally localized Wannier functions (MLWFs) here provide an intuitive description of chemical bonding^{153,154} linked with the concept of valence bonds in chemistry. In trans-polyacetylene, two C=C, one C–C, and two C–H MLWFs can be identified in each monomer unit as shown in Figure 4b, and the dynamics of the topological pumping is governed by the Wannier center movement of both C=C double bonds and C–C single bonds but not of C–H bonds as seen in Figure 4c.⁵ While the double and single bond Wannier centers move in opposite directions, having more electrons in the double bonds than in the single bonds results in a net unidirectional transport overall. This interpretation of the topological property in terms of the valence bond model can be used to predict the emergence of the Floquet topological phase with respect to molecular changes to trans-polyacetylene as discussed in detail in ref 138.

TDDFT is gauge-invariant with respect to the unitary transformation of the time-dependent KS orbitals such that the underlying quantum dynamics remain unchanged. In the so-called dynamical transition orbital (DTO) gauge,⁹⁰ the nonadiabatic Thouless pumping can be represented in terms of minimal particle-hole transitions. The DTOs are obtained through the unitary transformation such that each DTO is given by a pair of the hole and particle orbitals (i.e., $| \psi_n^{\text{DTO}}(t) \rangle = h_n(t) | \psi_n^{\text{hole}}(t) \rangle + p_n(t) | \psi_n^{\text{particle}}(t) \rangle$). The real-valued positive expansion coefficients satisfy $h_n(t)^2 + p_n(t)^2 = 1$, and the particle/hole orbitals are obtained from the unoccupied/occupied eigenstates of the system at equilibrium. Figure 5a shows how the particle population, $p_n(t)$, changes in time for the three DTOs with the most dominant changes in the case of the Floquet topological phase with $W = 1$. In this minimal transition representation, the quantum dynamics responsible for the topological pumping largely manifest in the time-dependent changes of a single DTO orbital (i.e., $\Delta\rho(\mathbf{r}, t) \approx |\Delta\phi_1^{\text{DTO}}(\mathbf{r}, t)|^2$). Figure 5b shows how this particular DTO orbital changes from having π bonding character to acquiring π^* antibonding character of the molecular orbital theory.⁵ The RT-TDDFT simulation here allows us to connect the nonadiabatic Thouless pumping to these familiar concepts in chemistry. Topological matter has become a very active topic of research in the past decade, and RT-TDDFT simulation can contribute greatly to its development, especially for connecting various model Hamiltonian descriptions to real chemical systems. There are growing efforts to develop a molecular-level understanding of topological materials from the perspective of chemistry,^{155,156} and the gauge transformation was utilized here to rationalize how the Floquet topological phase emerges in the framework of well-recognized chemistry concepts.¹³⁸ Although RT-TDDFT simulation provides fundamental molecular-level understanding, quantitative prediction of the specific conditions, such as the electric field amplitudes/frequencies, remains challenging. This is again largely due to the approximated nature of the XC potential used in practical RT-TDDFT simulations, and the “phase diagram” for the topological phase is certainly susceptible to the XC approximation. The ability to quantitatively predict the specific electric field needed for inducing the Floquet topological phase and guide experiments will require further advancement of TDDFT.

4. CHALLENGES AND FUTURE DEVELOPMENT

While RT-TDDFT has rapidly garnered great interest in recent years, especially for studying various nonequilibrium electron

dynamical phenomena, it is certainly not without outstanding challenges. The exchange-correlation (XC) approximation continues to be the key approximation in RT-TDDFT. Future development must also include theoretical/computational work on how various effects of the “environment” can be coupled to electron dynamics, as we aim to model increasingly more complex situations. While there are many exciting developments, we focus on a few key developments of particular relevance for chemistry here.

4.1. Advancing Exchange-Correlational Approximation. It was not until sufficiently accurate exchange-correlation (XC) approximations were developed that DFT became widely accepted in the chemistry community,¹⁵⁷ and the importance of XC approximation cannot be overstated. Like its ground-state counterpart, the accuracy of TDDFT is ultimately dependent on the XC approximation. For ground-state DFT calculations, the XC approximation has become increasingly sophisticated in recent years. Even those XC approximations that belong to the fifth-rung of the so-called DFT’s Jacob’s ladder¹⁵⁸ like the exact exchange (EXX) plus the random phase approximation (RPA)¹⁴⁰ have been employed for calculations of extended systems.^{159,160} Machine-learning techniques have also been increasingly used to devise sophisticated XC approximations in recent years.^{161–163} Another key approximation in practical RT-TDDFT simulations is that the XC potential depends only on the instantaneous electron density, using the XC approximations developed for the ground-state DFT while the true XC potential is a function of the electron density at all previous times in principle.¹⁶⁴ This so-called adiabatic approximation to the XC potential is widely adapted, but it is known to fail in describing certain types of electronic excitation, like those with the double-excitation character.^{165,166}

For applications of RT-TDDFT on extended systems, local and semilocal XC approximations remain most prevalent. Aside from the obvious benefit of having increasingly more quantitative predictions through the development of accurate XC approximations, RT-TDDFT simulations will benefit greatly from XC functionals suitable for modeling long-range charge transfer and exciton formation/dissociation in particular.¹⁶⁷ So-called hybrid XC functionals, in which a fraction of EXX is included,¹⁶⁸ have become a practical and promising approach in this regard. Screened range-separated¹⁶⁹ and dielectric-dependent^{170,171} hybrid XC approximations have emerged as a particularly interesting paradigm, and they could provide an alternative to the computationally expensive many-body Green’s function theory framework for studying excited-state properties. These advanced XC functionals likely lead to an accurate RT-TDDFT description of exciton dynamics in complex extended systems. Screened range-separated hybrid XC functionals have already been used in linear-response TDDFT, and excitonic features in the optical absorption spectrum were successfully modeled.^{172,173} Capturing excitonic features as well as an accurate description of long-range charge-transfer excitations typically lie beyond standard semilocal XC approximations. However, the use of hybrid XC functionals remains particularly difficult for studying extended systems with delocalized KS orbitals because of its prohibitively large computational cost, and such a difficulty is further compounded in RT-TDDFT simulation. Various numerical techniques have been devised to reduce the computational cost, often by taking advantage of the spatially localized nature of basis set functions.^{174–178} The orbital gauge invariance

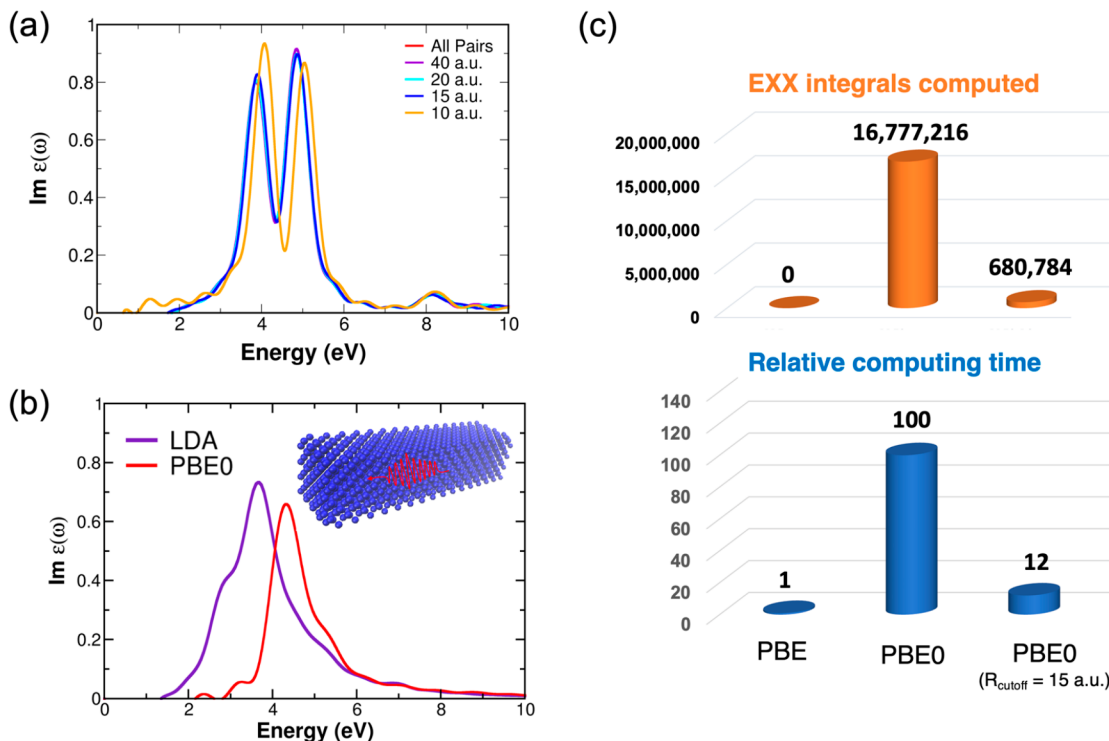


Figure 6. (a) Sensitivity of the calculated optical absorption spectrum with respect to the MLWF cutoff distance, R_{cutoff} , for PBE0 hybrid XC approximation. A small 512-electron simulation cell of crystalline silicon with periodic boundary conditions (PBCs) was used to determine the minimal necessary MLWF cutoff distance. An optical absorption spectrum can be calculated from the RT-TDDFT simulation of electron dynamics as discussed in ref 3. (b) An optical absorption spectrum of crystalline silicon according to the PBE0 hybrid XC approximation was obtained with a large simulation cell (8192 valence electrons) with the PBC. The result using the LDA XC approximation is shown for comparison. (c) The number of EXX integrals calculated is shown for PBE, PBE0, and PBE0 with the MLWF cutoff distance, $R_{\text{cutoff}} = 15$ bohr. The relative computational cost is also shown for these simulations performed on an ALCF-Theta machine using 32,768 processors (512 KNL nodes), and only MPI (no open-MP/SIMD) was used for the benchmarking purpose.

discussed in Section 2 can also be exploited to reduce the prohibitively large computational cost associated with EXX^{3,88,89} by noting that the unitary transformation of the time-dependent KS orbitals does not change the underlying quantum dynamics. This is particularly useful when the basis set functions are delocalized, as for the plane-waves, which are widely used to model extended systems in electronic structure theory. Our recent work,³ for example, describes that the computational cost of calculating the exchange integral is significantly reduced by expressing the EXX part of $\hat{v}_{\text{XC}}(\mathbf{r}, t)$ as

$$\hat{v}^{\text{EXX}}(t)w_i(\mathbf{r}, t) = -\sum_j \int d\mathbf{r}' \frac{w_j^*(\mathbf{r}', t)w_i(\mathbf{r}', t)}{|\mathbf{r} - \mathbf{r}'|} w_j(\mathbf{r}, t) \quad (6)$$

where $\{w_i(\mathbf{r}, t)\}$ are the spatially localized MLWFs that are propagated in the RT-TDDFT simulation. The EXX integral with the time-dependent MLWFs indexed with i and j is essentially zero if, for instance, the two MLWFs are located on different chemical motifs separated by several tens of Angstroms. The integral needs to be calculated only if the MLWFs are spatially close such that $|\langle w_i | \hat{r} | w_j \rangle - \langle w_i | \hat{r} | w_j \rangle| < R_{\text{cutoff}}$ where R_{cutoff} is a distance cutoff parameter. Since time-dependent MLWFs generally remain spatially localized even in RT-TDDFT simulations,² the integral does not need to be calculated for many MLWF pairs that are situated on different parts of the system. This reduction becomes increasingly more significant for large complex systems, due to the nearsightedness principle of electrons.¹⁷⁹ Such an idea has already been

employed for the ground-state DFT in the context of first-principles molecular dynamics simulation,^{180,181} and the approach works quite well also for RT-TDDFT. Figure 6 illustrates how the MLWF distance cutoff can be used to significantly reduce the computational cost for the calculation of the optical absorption spectrum of crystalline silicon as an example with the PBE0¹⁸² hybrid XC functional. A small simulation cell can be used to assess the sensitivity with respect to the MLWF distance cutoff, and Figure 6a shows that the spectrum does not change until the MLWF distance cutoff is reduced to less than 15 bohr. Using the cutoff distance of 15 bohr, we can compute the converged optical absorption spectrum of crystalline silicon using a large 2048-atom (8192 electrons) simulation cell, as shown in Figure 6b. Figure 6c shows that only 4.06% of all of the EXX integrals need to be calculated, and the overall computational cost is reduced significantly by an order of magnitude. Even with the massively parallel HPC we used here (Theta machine at Argonne National Laboratory, using 32,768 processors), such a large hybrid-XC RT-TDDFT simulation would have not been practical without the use of the MLWF distance cutoff approach.

Let us discuss how hybrid XC approximations improve the RT-TDDFT accuracy by using the description of electronic excitation as an example, particularly the excitonic effect. In the simplest approximation, we might neglect the quantum-mechanical interaction between the excited electron and the hole. At the same time, the interaction between the excited electron and the hole, often called the excitonic effect, can be

important in various situations, and accurate atomistic modeling of this quasi-particle, the exciton, with first-principles theory is of great interest. An infinite chain of elongated H₂ molecules is often used as a test case for modeling the excitonic effect in the optical absorption spectrum of an extended system.¹ Figure 7 shows the comparison of optical absorption

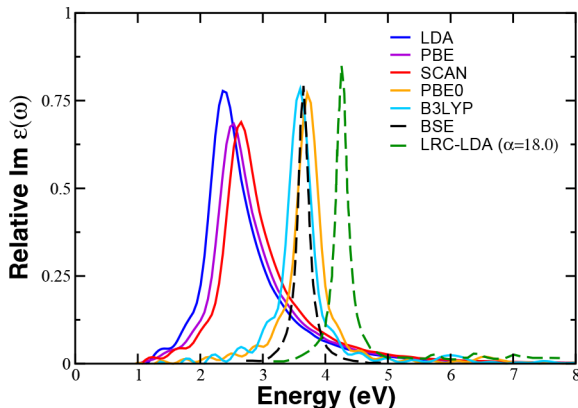


Figure 7. Optical absorption spectrum for the infinite chain of elongated H₂ (see ref 1 for more details), obtained from the RT-TDDFT simulation using several XC approximations. The simulation cell consists of 116 H₂ with periodic boundary conditions. We also show the BSE calculation with a GW quasiparticle energy shift⁹ and linear-response TDDFT calculation with the tuned long-range corrected kernel (LRC-LDA)¹ for comparison.⁹ For hybrid XC approximations, only 11% of the EXX integrals needed to be computed because MLWFs are propagated in the RT-TDDFT simulations. This made the computational cost with hybrid XC approximations only five times more expensive than that of GGA calculations.

spectra computed from a RT-TDDFT simulation using several popular XC approximations of different sophistications from the LDA to GGA (PBE),¹³⁴ meta-GGA (SCAN),^{183,184} and hybrid-GGAs (PBE0¹⁸² and B3LYP¹⁸⁵). The spectra are also compared to the linear-response TDDFT calculation using the long-range corrected (LRC) XC kernels^{1,186–188} and to the Bethe–Salpeter equation (BSE) calculation.^{189–191} The BSE is a many-body Green's function theory approach and is currently the state-of-the-art method for studying electronic excitation in condensed matter systems even though its large computational cost often prevents us from applying the calculation routinely. The BSE formalism explicitly takes into account the excitonic effect that derives from the quantum-mechanical interaction between the excited electron and hole. As seen in Figure 7, semilocal XC approximations like LDA, PBE, and SCAN erroneously yield a much broader absorption spectrum in addition to having the peak position red-shifted. The hybrid XC approximation, PBE0, greatly improves on these shortcomings, and a similar improvement is also observed for the B3LYP hybrid XC approximation.^{192,193} Recent advances, especially via the screened and dielectric-dependent hybrid XC framework,^{171–173} are likely to further improve the accuracy of DFT-related methodologies including RT-TDDFT simulation.

Alternatively to the hybrid XC methodology, incorporating the long-range screening of electron–hole interaction through the XC vector potential has also become a promising avenue for modeling exciton dynamics in RT-TDDFT.⁹ While such an approach has been successfully demonstrated within a linear-

response TDDFT calculation^{186,187} (e.g., see Figure 7), its adaptation in RT-TDDFT simulations was reported only recently by the groups of Schleife and Ullrich.⁹ The electronic current tends to become rather unstable due to the explicit dependence of the XC vector potential on the time-dependent current, and further advancement is needed before its widespread usage can be expected for practical application. Despite practical challenges, the TD current-DFT^{14,194–196} formulation provides a more general formalism of RT-TDDFT for remedying another important limitation, the adiabatic approximation to the XC effect.^{22,164,165} As mentioned briefly, a key approximation in practical RT-TDDFT simulations is that the XC potential depends on only the instantaneous electron density. Vignale and Kohn showed that the “history” dependence of the XC effect can be incorporated through the time-dependent current as a basic variable.¹⁹⁵ This formulation within the linear response theory was later extended to the mathematical form applicable to RT-TDDFT through the XC vector potential with the time-dependent current.^{197,198} Alleviating the adiabatic approximation for the XC potential remains a fundamental TDDFT topic of great importance,¹⁶⁵ and RT-TDDFT can potentially benefit greatly from new advances in TD current-DFT formulation.¹⁹⁹

4.2. Coupled Quantum Dynamics with Protons. While the positions of atomic nuclei are often held fixed in a RT-TDDFT simulation, it is straightforward to incorporate the nuclear movement with the so-called Ehrenfest dynamics approach.²⁰⁰ This approach can be employed with various electronic structure methods.²⁰¹ When it is used in conjunction with RT-TDDFT, the dynamics of the classical nuclei are governed by Newton's equation of motion and the forces on nuclei are obtained by calculating the gradient of DFT energy functional with respect to their positions. In this description, the Coulomb interaction with the time-dependent electron density is responsible for the forces. Although the Ehrenfest dynamics is a powerful and popular mixed quantum-classical dynamics method, some key physics are missing and some well-recognized phenomena cannot be properly modeled (e.g., the Joule heating).²⁰² Perhaps most imperative in chemistry, the dynamics of some light nuclei like those of protons sometimes require explicit quantum mechanical treatment. For studying concerted dynamical phenomena such as proton-coupled electron transfer (PCET) and excited-state proton transfer (ESPT), the quantum dynamical nature of protons can be important for obtaining a correct description. The Hohenberg–Kohn theorem has been formally extended in the so-called multicomponent DFT formalism such that more than one type of particle can be described as quantum particles without the Born–Oppenheimer approximation.^{203–205} This is a particularly powerful theoretical formulation because it naturally incorporates quantum-mechanical correlation among electrons and other nuclei like protons. In parallel, Hammes-Schiffer and co-workers developed the so-called nuclear electronic orbital (NEO) method such that electronic and nuclear degrees of freedom can be treated quantum-mechanically on an equal footing in electronic structure theory.^{206,207} The NEO method has been extended to the Kohn–Sham ansatz of DFT, making the multicomponent DFT a particularly practical approach for studying interesting phenomena in which both protons and electrons need to be treated quantum-mechanically. In this context, Yang et al. developed electron–proton correlation functionals via the Colle–Salvetti ansatz,^{208,209} and the

extension of NEO-DFT to the real-time propagation method by Li²⁶ and Hammes-Schiffer^{206,207} has further advanced the exciting realm of RT-TDDFT (RT-NEO-TDDFT). With reliable approximations for the electron–proton correlation functional along with further development for adapting the periodic boundary conditions to study extended systems,²¹¹ it is now possible to study coupled quantum dynamics of electrons and protons in complex chemical systems.⁸

Let us briefly discuss how such an RT-NEO-TDDFT methodology is opening up a new research direction through an example. Excited-state intramolecular proton transfer (ESIPT) is a prototypical class of chemical dynamics in which quantum-mechanical proton transfer is induced by electronic excitation in a molecule. Intramolecular proton transfer in an *o*-hydroxybenzaldehyde (*o*HBA) molecule has been studied as a classic example of ESIPT, including via the RT-NEO-TDDFT approach.²¹⁰ New advances further enable us to examine how nonequilibrium electron dynamics impact the ESIPT process when the molecule is part of a complex heterogeneous environment like being chemisorbed at a semiconductor surface.^{8,211} The initial electronic excitation, modeled here by simply promoting an electron from HOMO to LUMO of the *o*HBA molecule, causes the quantum-mechanical proton to transfer between two oxygen atoms (O_D and O_A) on the femtosecond time scale as discussed in ref 210 (see Figure 8a). When the molecule is adsorbed on an H-

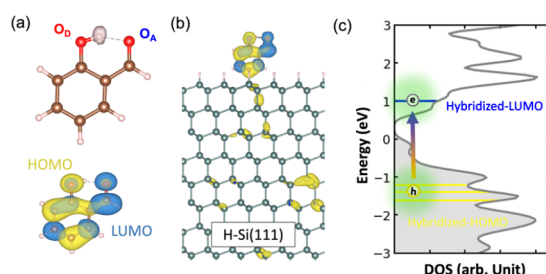


Figure 8. (a) The *o*-hydroxybenzaldehyde (*o*HBA) molecule which exhibits ultrafast intramolecular proton transfer upon HOMO–LUMO electronic excitation. Blue and yellow isosurface plots show the LUMO and HOMO, respectively. (b) *o*HBA adsorbed directly on a H–Si(111) semiconductor surface. Hybridized HOMO and LUMO are also shown. (c) Electronic density of states for the interfaced system of *o*HBA adsorbed directly on the H–Si(111) surface. At $t = 0$ in the RT-NEO-TDDFT simulation, an electron is manually promoted from one of the three hybridized HOMOs to the hybridized LUMO. Adapted with permission from ref 8. Copyright 2023 the American Physical Society.

Si(111) surface, the orbital hybridization results in having three KS eigenstates with an appreciable molecular HOMO character and only one KS eigenstate with significant molecular LUMO character, as shown in Figure 8b,c. Even when a $-\text{C}\equiv\text{C}-$ linker group is inserted between the *o*HBA molecule and the Si(111) surface (instead of directly chemisorbed), this electronic structure description does not change. Mulliken charge analysis shows that more than 80% of the hybridized LUMO is spatially localized on the molecule while each hybridized HOMO shows only about 20% on the molecule. In the RT-NEO-TDDFT simulation, an electron is promoted from one of the three hybridized HOMOs to the hybridized LUMO at the beginning of the simulation (i.e., $t = 0$) as depicted in Figure 8c. Figure 9a shows the distances between the position expectation value of the quantum proton to the

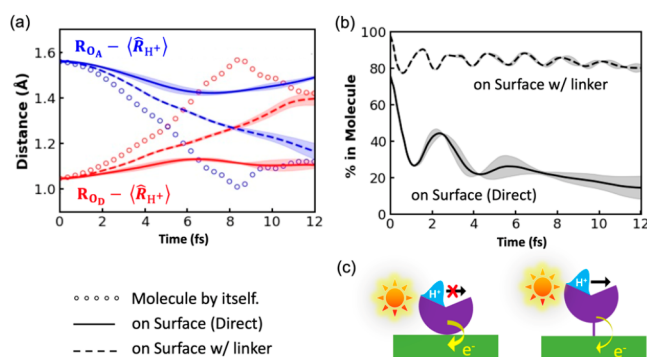


Figure 9. RT-NEO-TDDFT simulation of *o*HBA on the H–Si(111) surface with and without a $-\text{C}\equiv\text{C}-$ linker between the *o*HBA molecule and the surface. (a) The distances between the position expectation value of the quantum proton to the accepting (O_A) and donating (O_D) oxygen atoms in *o*HBA. The comparison to the result for the molecule in the gas phase is also shown. (b) Fraction of the excited electron in the *o*HBA molecule, according to the Mulliken population analysis. (c) Schematics of how the linker group impacts the interfacial excited electron transfer and the intramolecular proton transfer. Adapted with permission from ref 8. Copyright 2023 the American Physical Society.

accepting (O_A) and donating (O_D) oxygen atoms (see Figure 8a). The proton transfer does not take place when the molecule is directly adsorbed on the surface, while the proton transfer still takes place when the linker group is present. Figure 9b shows the time-dependent probability amplitude of the excited electron within the *o*HBA molecule. When the molecule is directly bonded to the surface, the excited electron quickly transfers to the semiconductor surface on the same time scale as the proton transfer. However, the excited electron largely remains within the molecule on that time scale when the molecule is adsorbed with the linker group and situated farther away from the surface. Even for the ultrafast proton transfer here, the time scale of the interfacial excited electron transfer is comparatively fast in the direct attachment case and the driving force for the proton transfer rapidly diminished as schematically depicted in Figure 9c. In summary, the RT-NEO-TDDFT simulation of the coupled quantum dynamics of electrons and protons enabled us to study the competition between the interfacial excited electron transfer and proton transfer from first principles.⁸ This type of RT-TDDFT simulation in which protons are quantized via the NEO method opens an exciting new research direction, and understanding such coupled quantum dynamics of protons and electrons in heterogeneous systems is particularly important in the context of the CO_2 reduction reaction at molecular-functionalized photocathodes as pursued in the DOE Energy Innovation Hub: Center for Hybrid Approaches in Solar Energy to Liquid Fuels (CHASE).²¹²

Quantum dynamics of nuclei, particularly of protons, is receiving great attention nowadays in general. The NEO method is certainly not the only formalism that we can employ for RT-TDDFT simulation. Meng and co-workers recently extended the RT-TDDFT simulation with a path-integral representation for nuclei²¹³ via ring-polymer molecular dynamics.^{214–216} They have successfully applied this method to study the ultrafast proton transfer in liquid water, as it is experimentally observed with the ionization of water molecules. They found that the quantum nature of the proton is essential to ultrafast proton transfer. Exact factorization is

another emerging formalism that enables incorporation of nuclear quantum dynamics. The general formulation of the exact factorization was introduced in 2010 by Gross and co-workers,²¹⁷ and it has also been extended in the context of DFT.²¹⁸ Their work has shown that the total multicomponent wave function can be expressed as a simple product of a nuclear wave function and a conditional electronic wave function. These two wave functions are coupled via additional effective vector and scalar potentials in their respective Hamiltonians for the nuclear and electronic degrees of freedom. While the exact factorization has not been extensively used to study the dynamics of complex chemical systems, this formalism is also promising for simulating coupled quantum dynamics within RT-TDDFT framework.^{219,220}

5. CONCLUDING REMARK AND FUTURE OUTLOOK

Time-dependent density functional theory (TDDFT) has become the first-principles method of choice for studying various electronic excitation properties of a wide range of systems from molecules to condensed phase systems such as liquids and solids. In particular, the linear response theory formulation of TDDFT has garnered great popularity for calculating the optical properties of molecules. At the same time, new advances in computational methods and the availability of increasingly powerful computing hardware have facilitated the growing popularity of the explicit real-time propagation approach for TDDFT (RT-TDDFT) in the last few decades. In addition to studying nonlinear effects in photoexcitation, RT-TDDFT is used to study various non-equilibrium electron dynamics phenomena. In this Perspective, we discussed studies on the electronic stopping of DNA in water and the emergence of the Floquet topological phase in molecular systems as examples of how RT-TDDFT simulations have enabled us to gain new scientific understandings. Recent advances have made it possible to simulate non-equilibrium electron dynamics in complex chemical systems from first-principles, and this new computational paradigm offers an exciting alternative to the traditional approach to quantum dynamics with model Hamiltonians.

Despite its great success in recent years, the RT-TDDFT method is certainly not without outstanding challenges. RT-TDDFT simulations are not free from the same challenges that DFT practitioners continue to face concerning the exchange-correlation (XC) approximation. In addition to accuracy, the efficiency of approximated XC functionals is an important practical consideration for computationally expensive RT-TDDFT simulations. Additionally, the history-memory dependence of the XC approximation remains a challenging question for TDDFT and is particularly difficult to handle in RT-TDDFT simulations. For RT-TDDFT to contribute to greater scientific impacts by studying increasingly complex systems and phenomena, future development must also include theoretical/computational work on incorporating various effects of the “environment” in explicit electron dynamics. In this Perspective, we discussed the coupled quantum dynamics of electrons with protons as an example in this direction. Modeling the quantum nature of photons^{221,222} and macroscopic electromagnetic fields²²³ with the nonequilibrium electron dynamics is another important direction for RT-TDDFT simulation. Coupling with phonons/vibrations is another important consideration, as it is largely responsible for the relaxation/thermalization of excited electrons, which usually takes place over picoseconds or even longer. While

the surface hopping method²²⁴ has been combined with the quantum dynamics simulation in the KS single-particle picture with great success,^{225,226} direct RT-TDDFT simulation of such a long time scale process is computationally impractical in most cases. An emerging use of machine learning for quantum dynamics simulation^{227,228} can potentially alleviate this time scale problem for RT-TDDFT simulations in the future. Another challenge in describing this type of coupling is the decoherence/dephasing effect due to nuclear dynamics.^{229,230} Under certain approximations, it is possible to incorporate the decoherence effect even in the mixed quantum-classical dynamics methods by calculating the decoherence rate from first principles.^{231–233} At the same time, accounting for the decoherence directly within the RT-TDDFT simulation remains an active area of research.^{234–236} There are many outstanding and exciting challenges for RT-TDDFT, and they continue to require active computational and theoretical development in the field.

■ AUTHOR INFORMATION

Corresponding Author

Yosuke Kanai — Department of Chemistry and Department of Physics and Astronomy, University of North Carolina at Chapel Hill, Chapel Hill, North Carolina 27599, United States;  orcid.org/0000-0002-2320-4394; Email: ykanai@unc.edu

Authors

Jianhang Xu — Department of Chemistry, University of North Carolina at Chapel Hill, Chapel Hill, North Carolina 27599, United States;  orcid.org/0000-0002-6253-6201

Thomas E. Carney — Department of Chemistry, University of North Carolina at Chapel Hill, Chapel Hill, North Carolina 27599, United States

Ruiyi Zhou — Department of Chemistry, University of North Carolina at Chapel Hill, Chapel Hill, North Carolina 27599, United States;  orcid.org/0000-0002-7732-6338

Christopher Shepard — Department of Chemistry, University of North Carolina at Chapel Hill, Chapel Hill, North Carolina 27599, United States;  orcid.org/0000-0002-3604-414X

Complete contact information is available at:
<https://pubs.acs.org/10.1021/jacs.3c08226>

Notes

The authors declare no competing financial interest.

■ ACKNOWLEDGMENTS

This work was partially supported by the National Science Foundation under Award Nos. CHE-1954894 and OAC-2209858 for the development of RT-TDDFT methodologies. This work was also partially supported as part of the Center for Hybrid Approaches in Solar Energy to Liquid Fuels (CHASE), an Energy Innovation Hub funded by the U.S. Department of Energy, Office of Science, Office of Basic Energy Sciences under Award Number DE-SC0021173 for the development of the nuclear-electronic orbital method in RT-TDDFT for modeling quantum dynamics of protons. We thank the Research Computing at the University of North Carolina at Chapel Hill for computer resources. An award of computer time was also provided by the Innovative and Novel Computational Impact on Theory and Experiment (INCITE) program. This research used resources of the Argonne

Leadership Computing Facility (ALCF), which is a DOE Office of Science User Facility supported under Contract No. DE-AC02-06CH11357.

■ REFERENCES

- (1) Byun, Y.-M.; Ullrich, C. A. Assessment of long-range-corrected exchange-correlation kernels for solids: Accurate exciton binding energies via an empirically scaled bootstrap kernel. *Phys. Rev. B* **2017**, *95* (20), 205136.
- (2) Yost, D. C.; Yao, Y.; Kanai, Y. Propagation of maximally localized Wannier functions in real-time TDDFT. *J. Chem. Phys.* **2019**, *150* (19), 194113.
- (3) Shepard, C.; Zhou, R.; Yost, D. C.; Yao, Y.; Kanai, Y. Simulating electronic excitation and dynamics with real-time propagation approach to TDDFT within plane-wave pseudopotential formulation. *J. Chem. Phys.* **2021**, *155* (10), 100901.
- (4) Yao, Y.; Yost, D. C.; Kanai, Y. \$K\$-Shell Core-Electron Excitations in Electronic Stopping of Protons in Water from First Principles. *Phys. Rev. Lett.* **2019**, *123* (6), No. 066401.
- (5) Zhou, R.; Yost, D. C.; Kanai, Y. First-Principles Demonstration of Nonadiabatic Thouless Pumping of Electrons in a Molecular System. *J. Phys. Chem. Lett.* **2021**, *12*, 4496–4503.
- (6) Shimizu, M.; Kaneda, M.; Hayakawa, T.; Tsuchida, H.; Itoh, A. Stopping cross sections of liquid water for MeV energy protons. *Nuclear Instruments and Methods in Physics Research Section B: Beam Interactions with Materials and Atoms* **2009**, *267* (16), 2667–2670.
- (7) Shimizu, M.; Hayakawa, T.; Kaneda, M.; Tsuchida, H.; Itoh, A. Stopping cross-sections of liquid water for 0.3–2.0 MeV protons. *Vacuum* **2010**, *84* (8), 1002–1004.
- (8) Xu, J.; Zhou, R.; Blum, V.; Li, T. E.; Hammes-Schiffer, S.; Kanai, Y. First-Principles Approach for Coupled Quantum Dynamics of Electrons and Protons in Heterogeneous Systems. *Phys. Rev. Lett.* **2023**, *131* (23), 238002.
- (9) Sun, J.; Lee, C.-W.; Kononov, A.; Schleife, A.; Ullrich, C. A. Real-Time Exciton Dynamics with Time-Dependent Density-Functional Theory. *Phys. Rev. Lett.* **2021**, *127* (7), No. 077401.
- (10) Shepard, C.; Yost, D. C.; Kanai, Y. Electronic Excitation Response of DNA to High-Energy Proton Radiation in Water. *Phys. Rev. Lett.* **2023**, *130* (11), 118401.
- (11) Car, R.; Parrinello, M. Unified Approach for Molecular Dynamics and Density-Functional Theory. *Phys. Rev. Lett.* **1985**, *55* (22), 2471–2474.
- (12) Hutter, J. Car–Parrinello molecular dynamics. *WIREs Computational Molecular Science* **2012**, *2* (4), 604–612.
- (13) Runge, E.; Gross, E. K. U. Density-Functional Theory for Time-Dependent Systems. *Phys. Rev. Lett.* **1984**, *52* (12), 997–1000.
- (14) Ullrich, C. A. *Time-Dependent Density-Functional Theory, Concepts and Applications*; Oxford University Press, 2011.
- (15) Casida, M. Time-dependent density-functional response theory for molecules. In *Recent Advances in Density Functional Methods, Part I*; World Scientific: Singapore, 1995.
- (16) Petersilka, M.; Gossmann, U. J.; Gross, E. K. U. Excitation Energies from Time-Dependent Density-Functional Theory. *Phys. Rev. Lett.* **1996**, *76* (8), 1212–1215.
- (17) Walker, B.; Saitta, A. M.; Gebauer, R.; Baroni, S. Efficient Approach to Time-Dependent Density-Functional Perturbation Theory for Optical Spectroscopy. *Phys. Rev. Lett.* **2006**, *96* (11), 113001.
- (18) Burke, K.; Werschnik, J.; Gross, E. K. U. Time-dependent density functional theory: Past, present, and future. *J. Chem. Phys.* **2005**, *123* (6), No. 062206.
- (19) Casida, M. E.; Huix-Rotllant, M. Progress in Time-Dependent Density-Functional Theory. *Annu. Rev. Phys. Chem.* **2012**, *63* (1), 287–323.
- (20) Ullrich, C. A.; Yang, Z. -h. A Brief Compendium of Time-Dependent Density Functional Theory. *Brazilian Journal of Physics* **2014**, *44* (1), 154–188.
- (21) Marques, M. A. L.; Gross, E. K. U. TIME-DEPENDENT DENSITY FUNCTIONAL THEORY. *Annu. Rev. Phys. Chem.* **2004**, *55* (1), 427–455.
- (22) Marques, M.; Maitra, N.; Nogueira, F.; Gross, E. K. U.; Rubio, A. *Fundamentals of Time-Dependent Density Functional Theory*; Springer, 2012.
- (23) Marques, M. A. L.; Ullrich, C. A.; Nogueira, F.; Rubio, A.; Burke, K.; Gross, E. K. U. *Time-Dependent Density Functional Theory*; Springer: Germany, 2006.
- (24) Devi, K. R. S.; Koonin, S. E. Mean-Field Approximation to $p + He$ Scattering. *Phys. Rev. Lett.* **1981**, *47* (1), 27–30.
- (25) Meyer, H. D.; Manthe, U.; Cederbaum, L. S. The multi-configurational time-dependent Hartree approach. *Chem. Phys. Lett.* **1990**, *165* (1), 73–78.
- (26) Li, X.; Govind, N.; Isborn, C.; DePrince, A. E.; Lopata, K. Real-Time Time-Dependent Electronic Structure Theory. *Chem. Rev.* **2020**, *120* (18), 9951–9993.
- (27) Yabana, K.; Bertsch, G. F. Time-dependent local-density approximation in real time. *Phys. Rev. B* **1996**, *54* (7), 4484–4487.
- (28) Yabana, K.; Bertsch, G. F. Time-dependent local-density approximation in real time: Application to conjugated molecules. *Int. J. Quantum Chem.* **1999**, *75* (1), 55–66.
- (29) Theilhaber, J. Ab initio simulations of sodium using time-dependent density-functional theory. *Phys. Rev. B* **1992**, *46* (20), 12990–13003.
- (30) Lopata, K.; Govind, N. Modeling Fast Electron Dynamics with Real-Time Time-Dependent Density Functional Theory: Application to Small Molecules and Chromophores. *J. Chem. Theory Comput.* **2011**, *7* (5), 1344–1355.
- (31) Provorse, M. R.; Isborn, C. M. Electron dynamics with real-time time-dependent density functional theory. *Int. J. Quantum Chem.* **2016**, *116* (10), 739–749.
- (32) Goings, J. J.; Lestrage, P. J.; Li, X. Real-time time-dependent electronic structure theory. *Wiley Interdisciplinary Reviews: Computational Molecular Science* **2018**, *8* (1), e1341.
- (33) Castro, A.; Marques, M. A. L.; Alonso, J. A.; Bertsch, G. F.; Rubio, A. Excited states dynamics in time-dependent density functional theory. *European Physical Journal D - Atomic, Molecular, Optical and Plasma Physics* **2004**, *28* (2), 211–218.
- (34) Liang, W.; Chapman, C. T.; Li, X. Efficient first-principles electronic dynamics. *J. Chem. Phys.* **2011**, *134* (18), 184102.
- (35) Wachter, G.; Lemell, C.; Burgdörfer, J.; Sato, S. A.; Tong, X.-M.; Yabana, K. Ab Initio Simulation of Electrical Currents Induced by Ultrafast Laser Excitation of Dielectric Materials. *Phys. Rev. Lett.* **2014**, *113* (8), No. 087401.
- (36) Lian, C.; Guan, M.; Hu, S.; Zhang, J.; Meng, S. Photoexcitation in Solids: First-Principles Quantum Simulations by Real-Time TDDFT. *Advanced Theory and Simulations* **2018**, *1* (8), 1800055.
- (37) Senanayake, R. D.; Lingerfelt, D. B.; Kuda-Singappulige, G. U.; Li, X.; Aikens, C. M. Real-Time TDDFT Investigation of Optical Absorption in Gold Nanowires. *J. Phys. Chem. C* **2019**, *123* (23), 14734–14745.
- (38) Marques, M. A. L.; López, X.; Varsano, D.; Castro, A.; Rubio, A. Time-Dependent Density-Functional Approach for Biological Chromophores: The Case of the Green Fluorescent Protein. *Phys. Rev. Lett.* **2003**, *90* (25), 258101.
- (39) Schultze, M.; Ramasesha, K.; Pemmaraju, C. D.; Sato, S. A.; Whitmore, D.; Gandman, A.; Prell, J. S.; Borja, L. J.; Prendergast, D.; Yabana, K.; Neumark, D. M.; Leone, S. R. Attosecond band-gap dynamics in silicon. *Science* **2014**, *346* (6215), 1348.
- (40) Tussupbayev, S.; Govind, N.; Lopata, K.; Cramer, C. J. Comparison of Real-Time and Linear-Response Time-Dependent Density Functional Theories for Molecular Chromophores Ranging from Sparse to High Densities of States. *J. Chem. Theory Comput.* **2015**, *11* (3), 1102–1109.
- (41) Falke, S. M.; Rozzi, C. A.; Brida, D.; Maiuri, M.; Amato, M.; Sommer, E.; De Sio, A.; Rubio, A.; Cerullo, G.; Molinari, E.; Lienau, C. Coherent ultrafast charge transfer in an organic photovoltaic blend. *Science* **2014**, *344* (6187), 1001.

- (42) Meng, S.; Kaxiras, E. Electron and Hole Dynamics in Dye-Sensitized Solar Cells: Influencing Factors and Systematic Trends. *Nano Lett.* **2010**, *10* (4), 1238–1247.
- (43) Hatcher, R.; Beck, M.; Tackett, A.; Pantelides, S. T. Dynamical Effects in the Interaction of Ion Beams with Solids. *Phys. Rev. Lett.* **2008**, *100* (10), 103201.
- (44) Yost, D. C.; Yao, Y.; Kanai, Y. First-Principles Modeling of Electronic Stopping in Complex Matter under Ion Irradiation. *J. Phys. Chem. Lett.* **2020**, *11* (1), 229–237.
- (45) Prunedo, J. M.; Sánchez-Portal, D.; Arnau, A.; Juaristi, J. I.; Artacho, E. Electronic Stopping Power in LiF from First Principles. *Phys. Rev. Lett.* **2007**, *99* (23), 235501.
- (46) Correa, A. A.; Kohanoff, J.; Artacho, E.; Sánchez-Portal, D.; Caro, A. Nonadiabatic Forces in Ion-Solid Interactions: The Initial Stages of Radiation Damage. *Phys. Rev. Lett.* **2012**, *108* (21), 213201.
- (47) Schleife, A.; Kanai, Y.; Correa, A. A. Accurate atomistic first-principles calculations of electronic stopping. *Phys. Rev. B* **2015**, *91* (1), No. 014306.
- (48) Yost, D. C.; Yao, Y.; Kanai, Y. Examining real-time time-dependent density functional theory nonequilibrium simulations for the calculation of electronic stopping power. *Phys. Rev. B* **2017**, *96* (11), 115134.
- (49) Reeves, K. G.; Yao, Y.; Kanai, Y. Electronic stopping power in liquid water for protons and alpha particles from first principles. *Phys. Rev. B* **2016**, *94* (4), No. 041108.
- (50) Yost, D. C.; Kanai, Y. Electronic stopping for protons and alpha particles from first-principles electron dynamics: The case of silicon carbide. *Phys. Rev. B* **2016**, *94* (11), 115107.
- (51) Yost, D. C.; Kanai, Y. Electronic Excitation Dynamics in DNA under Proton and α -Particle Irradiation. *J. Am. Chem. Soc.* **2019**, *141* (13), 5241–5251.
- (52) Wang, Z.; Li, S.-S.; Wang, L.-W. Efficient Real-Time Time-Dependent Density Functional Theory Method and its Application to a Collision of an Ion with a 2D Material. *Phys. Rev. Lett.* **2015**, *114* (6), No. 063004.
- (53) Lopata, K.; Van Kuiken, B. E.; Khalil, M.; Govind, N. Linear-Response and Real-Time Time-Dependent Density Functional Theory Studies of Core-Level Near-Edge X-Ray Absorption. *J. Chem. Theory Comput.* **2012**, *8* (9), 3284–3292.
- (54) Pemmaraju, C. D.; Vila, F. D.; Kas, J. J.; Sato, S. A.; Rehr, J. J.; Yabana, K.; Prendergast, D. Velocity-gauge real-time TDDFT within a numerical atomic orbital basis set. *Comput. Phys. Commun.* **2018**, *226*, 30–38.
- (55) Attar, A. R.; Bhattacherjee, A.; Pemmaraju, C. D.; Schnorr, K.; Closser, K. D.; Prendergast, D.; Leone, S. R. Femtosecond x-ray spectroscopy of an electrocyclic ring-opening reaction. *Science* **2017**, *356* (6333), 54.
- (56) Pemmaraju, C. D. Valence and core excitons in solids from velocity-gauge real-time TDDFT with range-separated hybrid functionals: An LCAO approach. *Computational Condensed Matter* **2019**, *18*, No. e00348.
- (57) Goings, J. J.; Li, X. An atomic orbital based real-time time-dependent density functional theory for computing electronic circular dichroism band spectra. *J. Chem. Phys.* **2016**, *144* (23), 234102.
- (58) Peng, B.; Lingerfelt, D. B.; Ding, F.; Aikens, C. M.; Li, X. Real-Time TDDFT Studies of Exciton Decay and Transfer in Silver Nanowire Arrays. *J. Phys. Chem. C* **2015**, *119* (11), 6421–6427.
- (59) Ma, J.; Wang, Z.; Wang, L.-W. Interplay between plasmon and single-particle excitations in a metal nanocluster. *Nat. Commun.* **2015**, *6* (1), 10107.
- (60) Moss, C. L.; Isborn, C. M.; Li, X. Ehrenfest dynamics with a time-dependent density-functional-theory calculation of lifetimes and resonant widths of charge-transfer states of Li^+ near an aluminum cluster surface. *Phys. Rev. A* **2009**, *80* (2), No. 024503.
- (61) Isborn, C. M.; Li, X.; Tully, J. C. Time-dependent density functional theory Ehrenfest dynamics: Collisions between atomic oxygen and graphite clusters. *J. Chem. Phys.* **2007**, *126* (13), 134307.
- (62) Mrudul, M. S.; Tancogne-Dejean, N.; Rubio, A.; Dixit, G. High-harmonic generation from spin-polarised defects in solids. *npj Computational Materials* **2020**, *6* (1), 10.
- (63) Tancogne-Dejean, N.; Mücke, O. D.; Kärtner, F. X.; Rubio, A. Impact of the Electronic Band Structure in High-Harmonic Generation Spectra of Solids. *Phys. Rev. Lett.* **2017**, *118* (8), No. 087403.
- (64) Miyamoto, Y.; Zhang, H.; Cheng, X.; Rubio, A. Modeling of laser-pulse induced water decomposition on two-dimensional materials by simulations based on time-dependent density functional theory. *Phys. Rev. B* **2017**, *96* (11), 115451.
- (65) Hübener, H.; Sentef, M. A.; De Giovannini, U.; Kemper, A. F.; Rubio, A. Creating stable Floquet–Weyl semimetals by laser-driving of 3D Dirac materials. *Nat. Commun.* **2017**, *8* (1), 1–8.
- (66) Shin, D.; Sato, S. A.; Hübener, H.; De Giovannini, U.; Kim, J.; Park, N.; Rubio, A. Unraveling materials Berry curvature and Chern numbers from real-time evolution of Bloch states. *Proc. Natl. Acad. Sci. U. S. A.* **2019**, *116* (10), 4135.
- (67) Valiev, M.; Bylaska, E. J.; Govind, N.; Kowalski, K.; Straatsma, T. P.; Van Dam, H. J. J.; Wang, D.; Nieplocha, J.; Apra, E.; Windus, T. L.; de Jong, W. A. NWChem: A comprehensive and scalable open-source solution for large scale molecular simulations. *Comput. Phys. Commun.* **2010**, *181* (9), 1477–1489.
- (68) Takimoto, Y.; Vila, F. D.; Rehr, J. J. Real-time time-dependent density functional theory approach for frequency-dependent nonlinear optical response in photonic molecules. *J. Chem. Phys.* **2007**, *127* (15), 154114.
- (69) Soler, J. M.; Artacho, E.; Gale, J. D.; García, A.; Junquera, J.; Ordejón, P.; Sánchez-Portal, D. The SIESTA method for ab initio order-N materials simulation. *J. Phys.: Condens. Matter* **2002**, *14* (11), 2745–2779.
- (70) Kunert, T.; Schmidt, R. Non-adiabatic quantum molecular dynamics: General formalism and case study H_2^+ in strong laser fields. *European Physical Journal D - Atomic, Molecular, Optical and Plasma Physics* **2003**, *25* (1), 15–24.
- (71) Kühne, T. D.; Iannuzzi, M.; Del Ben, M.; Rybkin, V. V.; Seewald, P.; Stein, F.; Laino, T.; Khalil, R. Z.; Schütt, O.; Schiffmann, F.; Golze, D.; Wilhelm, J.; Chulkov, S.; Bani-Hashemian, M. H.; Weber, V.; Borštník, U.; Taillefumier, M.; Jakobovits, A. S.; Lazzaro, A.; Pabst, H.; Müller, T.; Schade, R.; Guidon, M.; Andermatt, S.; Holmberg, N.; Schenter, G. K.; Hehn, A.; Bussy, A.; Belleflamme, F.; Tabacchi, G.; Glöß, A.; Lass, M.; Bethune, I.; Mundt, C. J.; Plessl, C.; Watkins, M.; VandeVondele, J.; Krack, M.; Hutter, J. CP2K: An electronic structure and molecular dynamics software package - Quickstep: Efficient and accurate electronic structure calculations. *J. Chem. Phys.* **2020**, *152* (19), 194103.
- (72) Noda, M.; Sato, S. A.; Hirokawa, Y.; Uemoto, M.; Takeuchi, T.; Yamada, S.; Yamada, A.; Shinohara, Y.; Yamaguchi, M.; Iida, K.; Floss, I.; Otobe, T.; Lee, K.-M.; Ishimura, K.; Boku, T.; Bertsch, G. F.; Nobusada, K.; Yabana, K. SALMON: Scalable Ab-initio Light–Matter simulator for Optics and Nanoscience. *Comput. Phys. Commun.* **2019**, *235*, 356–365.
- (73) Marques, M. A. L.; Castro, A.; Bertsch, G. F.; Rubio, A. octopus: a first-principles tool for excited electron–ion dynamics. *Comput. Phys. Commun.* **2003**, *151* (1), 60–78.
- (74) Tancogne-Dejean, N.; Oliveira, M. J. T.; Andrade, X.; Appel, H.; Borca, C. H.; Le Breton, G.; Buchholz, F.; Castro, A.; Corni, S.; Correa, A. A.; De Giovannini, U.; Delgado, A.; Eich, F. G.; Flick, J.; Gil, G.; Gomez, A.; Helbig, N.; Hübener, H.; Jestädt, R.; Jornet-Somoza, J.; Larsen, A. H.; Lebedeva, I. V.; Lüders, M.; Marques, M. A. L.; Ohlmann, S. T.; Pipolo, S.; Rampp, M.; Rozzi, C. A.; Strubbe, D. A.; Sato, S. A.; Schäfer, C.; Theophilou, I.; Welden, A.; Rubio, A. Octopus, a computational framework for exploring light-driven phenomena and quantum dynamics in extended and finite systems. *J. Chem. Phys.* **2020**, *152* (12), 124119.
- (75) Nguyen, T. S.; Parkhill, J. Nonadiabatic Dynamics for Electrons at Second-Order: Real-Time TDDFT and OSCF2. *J. Chem. Theory Comput.* **2015**, *11* (7), 2918–2924.

- (76) Zhu, Y.; Herbert, J. M. Self-consistent predictor/corrector algorithms for stable and efficient integration of the time-dependent Kohn-Sham equation. *J. Chem. Phys.* **2018**, *148* (4), No. 044117.
- (77) Shao, Y.; Gan, Z.; Epifanovsky, E.; Gilbert, A. T. B.; Wormit, M.; Kussmann, J.; Lange, A. W.; Behn, A.; Deng, J.; Feng, X.; Ghosh, D.; Goldey, M.; Horn, P. R.; Jacobson, L. D.; Kaliman, I.; Khaliullin, R. Z.; Kuš, T.; Landau, A.; Liu, J.; Proynov, E. I.; Rhee, Y. M.; Richard, R. M.; Rohrdanz, M. A.; Steele, R. P.; Sundstrom, E. J.; Woodcock, H. L.; Zimmerman, P. M.; Zuev, D.; Albrecht, B.; Alguire, E.; Austin, B.; Beran, G. J. O.; Bernard, Y. A.; Berquist, E.; Brandhorst, K.; Bravaya, K. B.; Brown, S. T.; Casanova, D.; Chang, C.-M.; Chen, Y.; Chien, S. H.; Closser, K. D.; Crittenden, D. L.; Diedenhofen, M.; DiStasio, R. A.; Do, H.; Dutoi, A. D.; Edgar, R. G.; Fatehi, S.; Fusti-Molnar, L.; Ghysels, A.; Golubeva-Zadorozhnaya, A.; Gomes, J.; Hanson-Heine, M. W. D.; Harbach, P. H. P.; Hauser, A. W.; Hohenstein, E. G.; Holden, Z. C.; Jagau, T.-C.; Ji, H.; Kaduk, B.; Khistyayev, K.; Kim, J.; Kim, J.; King, R. A.; Klunzinger, P.; Kosenkov, D.; Kowalczyk, T.; Krauter, C. M.; Lao, K. U.; Laurent, A. D.; Lawler, K. V.; Levchenko, S. V.; Lin, C. Y.; Liu, F.; Livshits, E.; Lochan, R. C.; Luenser, A.; Manohar, P.; Manzer, S. F.; Mao, S.-P.; Mardirossian, N.; Marenich, A. V.; Maurer, S. A.; Mayhall, N. J.; Neuscamman, E.; Oana, C. M.; Olivares-Amaya, R.; O'Neill, D. P.; Parkhill, J. A.; Perrine, T. M.; Peverati, R.; Prociuk, A.; Rehn, D. R.; Rosta, E.; Russ, N. J.; Sharada, S. M.; Sharma, S.; Small, D. W.; Sodt, A.; Stein, T.; Stück, D.; Su, Y.-C.; Thom, A. J. W.; Tsuchimochi, T.; Vanovschi, V.; Vogt, L.; Vydrov, O.; Wang, T.; Watson, M. A.; Wenzel, J.; White, A.; Williams, C. F.; Yang, J.; Yeganeh, S.; Yost, S. R.; You, Z.-Q.; Zhang, I. Y.; Zhang, X.; Zhao, Y.; Brooks, B. R.; Chan, G. K. L.; Chipman, D. M.; Cramer, C. J.; Goddard, W. A.; Gordon, M. S.; Hehre, W. J.; Klamt, A.; Schaefer, H. F.; Schmidt, M. W.; Sherrill, C. D.; Truhlar, D. G.; Warshel, A.; Xu, X.; Aspuru-Guzik, A.; Baer, R.; Bell, A. T.; Besley, N. A.; Chai, J.-D.; Dreuw, A.; Dunietz, B. D.; Furlani, T. R.; Gwaltney, S. R.; Hsu, C.-P.; Jung, Y.; Kong, J.; Lambrecht, D. S.; Liang, W.; Ochsenfeld, C.; Rassolov, V. A.; Slipchenko, L. V.; Subotnik, J. E.; Van Voorhis, T.; Herbert, J. M.; Krylov, A. I.; Gill, P. M. W.; Head-Gordon, M. Advances in molecular quantum chemistry contained in the Q-Chem 4 program package. *Mol. Phys.* **2015**, *113* (2), 184–215.
- (78) Li, X.; Smith, S. M.; Markevitch, A. N.; Romanov, D. A.; Lewis, R. J.; Schlegel, H. B. A time-dependent Hartree–Fock approach for studying the electronic optical response of molecules in intense fields. *Phys. Chem. Chem. Phys.* **2005**, *7* (2), 233–239.
- (79) Maliyov, I.; Crocombe, J.-P.; Bruneval, F. Electronic stopping power from time-dependent density-functional theory in Gaussian basis. *European Physical Journal B* **2018**, *91* (8), 172.
- (80) Bruneval, F.; Rangel, T.; Hamed, S. M.; Shao, M.; Yang, C.; Neaton, J. B. MOLGW 1: Many-body perturbation theory software for atoms, molecules, and clusters. *Comput. Phys. Commun.* **2016**, *208*, 149–161.
- (81) Gygi, F. Architecture of qbox: A scalable first-principles molecular dynamics code. *IBM J. Res. Dev.* **2008**, *52*, 137–144.
- (82) Draeger, E. W.; Gygi, F. *Qbox code, Qb@ll version*; Lawrence Livermore National Laboratory.
- (83) Schleife, A.; Draeger, E. W.; Anisimov, V. M.; Correa, A. A.; Kanai, Y. Quantum Dynamics Simulation of Electrons in Materials on High-Performance Computers. *Computing in Science & Engineering* **2014**, *16* (5), 54–60.
- (84) Hekele, J.; Yao, Y.; Kanai, Y.; Blum, V.; Kratzer, P. All-electron real-time and imaginary-time time-dependent density functional theory within a numeric atom-centered basis function framework. *J. Chem. Phys.* **2021**, *155* (15), 154801.
- (85) Schleife, A.; Draeger, E. W.; Kanai, Y.; Correa, A. A. Plane-wave pseudopotential implementation of explicit integrators for time-dependent Kohn-Sham equations in large-scale simulations. *J. Chem. Phys.* **2012**, *137* (22), 22A546.
- (86) Castro, A.; Marques, M. A. L.; Rubio, A. Propagators for the time-dependent Kohn–Sham equations. *J. Chem. Phys.* **2004**, *121* (8), 3425–3433.
- (87) Gómez Pueyo, A.; Marques, M. A. L.; Rubio, A.; Castro, A. Propagators for the Time-Dependent Kohn–Sham Equations:
- Multistep, Runge–Kutta, Exponential Runge–Kutta, and Commutator Free Magnus Methods. *J. Chem. Theory Comput.* **2018**, *14* (6), 3040–3052.
- (88) Jia, W.; An, D.; Wang, L.-W.; Lin, L. Fast Real-Time Time-Dependent Density Functional Theory Calculations with the Parallel Transport Gauge. *J. Chem. Theory Comput.* **2018**, *14* (11), 5645–5652.
- (89) Jia, W.; Lin, L. Fast real-time time-dependent hybrid functional calculations with the parallel transport gauge and the adaptively compressed exchange formulation. *Comput. Phys. Commun.* **2019**, *240*, 21–29.
- (90) Zhou, R.; Kanai, Y. Dynamical transition orbitals: A particle–hole description in real-time TDDFT dynamics. *J. Chem. Phys.* **2021**, *154* (5), No. 054107.
- (91) Martin, R. L. Natural transition orbitals. *J. Chem. Phys.* **2003**, *118* (11), 4775–4777.
- (92) Marzari, N.; Mostofi, A. A.; Yates, J. R.; Souza, I.; Vanderbilt, D. Maximally localized Wannier functions: Theory and applications. *Rev. Mod. Phys.* **2012**, *84* (4), 1419–1475.
- (93) Donati, G.; Lingerfelt, D. B.; Aikens, C. M.; Li, X. Molecular Vibration Induced Plasmon Decay. *J. Phys. Chem. C* **2017**, *121* (28), 15368–15374.
- (94) Kumar, P. V.; Rossi, T. P.; Marti-Dafcik, D.; Reichmuth, D.; Kuisma, M.; Erhart, P.; Puska, M. J.; Norris, D. J. Plasmon-Induced Direct Hot-Carrier Transfer at Metal–Acceptor Interfaces. *ACS Nano* **2019**, *13* (3), 3188–3195.
- (95) Rossi, T. P.; Erhart, P.; Kuisma, M. Hot-Carrier Generation in Plasmonic Nanoparticles: The Importance of Atomic Structure. *ACS Nano* **2020**, *14* (8), 9963–9971.
- (96) Rozzi, C. A.; Troiani, F.; Tavernelli, I. Quantum modeling of ultrafast photoinduced charge separation. *J. Phys.: Condens. Matter* **2018**, *30* (1), No. 013002.
- (97) Race, C. P.; Mason, D. R.; Foo, M. H. F.; Foulkes, W. M. C.; Horsfield, A. P.; Sutton, A. P. Quantum–classical simulations of the electronic stopping force and charge on slow heavy channelling ions in metals. *J. Phys.: Condens. Matter* **2013**, *25* (12), 125501.
- (98) Bethe, H. Zur theorie des durchgangs schneller korpuskulärstrahlen durch materie. *Ann. Phys. (Berlin, Ger.)* **1930**, *397* (3), 325–400.
- (99) Lindhard, J. On the properties of a gas of charged particles. *Danske Matematisk-fysiske Meddeleiser* **1954**, *28*, 1–57.
- (100) Race, C. P.; Mason, D. R.; Finnis, M. W.; Foulkes, W. M. C.; Horsfield, A. P.; Sutton, A. P. The treatment of electronic excitations in atomistic models of radiation damage in metals. *Rep. Prog. Phys.* **2010**, *73* (11), 116501.
- (101) Correa, A. A. Calculating electronic stopping power in materials from first principles. *Comput. Mater. Sci.* **2018**, *150*, 291–303.
- (102) Shukri, A. A.; Bruneval, F.; Reining, L. Ab initio electronic stopping power of protons in bulk materials. *Phys. Rev. B* **2016**, *93* (3), No. 035128.
- (103) Zeb, M. A.; Kohanoff, J.; Sánchez-Portal, D.; Arnaud, A.; Juaristi, J. I.; Artacho, E. Electronic Stopping Power in Gold: The Role of d Electrons and the H/He Anomaly. *Phys. Rev. Lett.* **2012**, *108* (22), 225504.
- (104) Lee, C.-W.; Schleife, A. Electronic stopping and proton dynamics in InP, GaP, and In_{0.5}Ga_{0.5}P from first principles. The. *European Physical Journal B* **2018**, *91* (10), 222.
- (105) Ullah, R.; Artacho, E.; Correa, A. A. Core Electrons in the Electronic Stopping of Heavy Ions. *Phys. Rev. Lett.* **2018**, *121* (11), 116401.
- (106) Alvarez-Ibarra, A.; Parise, A.; Hasnaoui, K.; de la Lande, A. The physical stage of radiolysis of solvated DNA by high-energy-transfer particles: insights from new first principles simulations. *Phys. Chem. Chem. Phys.* **2020**, *22* (15), 7747–7758.
- (107) Stathakis, S. The Physics of Radiation Therapy. *Medical Physics* **2010**, *37*, 1374–1375.

- (108) Girdhani, S.; Sachs, R.; Hlatky, L. Biological Effects of Proton Radiation: What We Know and Don't Know. *Radiat. Res.* **2013**, *179* (3), 257–272.
- (109) Durante, M.; Loeffler, J. S. Charged particles in radiation oncology. *Nature Reviews Clinical Oncology* **2010**, *7* (1), 37–43.
- (110) Girdhani, S.; Sachs, R.; Hlatky, L. Biological Effects of Proton Radiation: What We Know and Don't Know. *Radiat. Res.* **2013**, *179* (3), 257–272.
- (111) Durante, M.; Loeffler, J. S. Charged particles in radiation oncology. *Nature reviews Clinical oncology* **2010**, *7* (1), 37.
- (112) Baskar, R.; Lee, K. A.; Yeo, R.; Yeoh, K.-W. Cancer and Radiation Therapy: Current Advances and Future Directions. *International Journal of Medical Sciences* **2012**, *9* (3), 193–199.
- (113) Girdhani, S.; Sachs, R.; Hlatky, L. Biological effects of proton radiation: what we know and don't know. *Radiat. Res.* **2013**, *179* (3), 257–72.
- (114) Vitti, E. T.; Parsons, J. L. The Radiobiological Effects of Proton Beam Therapy: Impact on DNA Damage and Repair. *Cancers* **2019**, *11* (7), 946.
- (115) Chaudhary, P.; Marshall, T. I.; Currell, F. J.; Kacperek, A.; Schettino, G.; Prise, K. M. Variations in the Processing of DNA Double-Strand Breaks Along 60-MeV Therapeutic Proton Beams. *Int. J. Radiat. Oncol. Biol. Phys.* **2016**, *95* (1), 86–94.
- (116) Loeffler, J. S.; Durante, M. Charged particle therapy—optimization, challenges and future directions. *Nature Reviews Clinical Oncology* **2013**, *10* (7), 411–424.
- (117) Shepard, C.; Kanai, Y. Nonlinear electronic excitation in water under proton irradiation: a first principles study. *Phys. Chem. Chem. Phys.* **2022**, *24* (9), 5598–5603.
- (118) Wong, J. C.; Kanai, Y. First Principles Dynamics Study of Excited Hole Relaxation in DNA. *ChemPhysChem* **2022**, *23* (1), e202100521.
- (119) Jones, B.; McMahon, S. J.; Prise, K. M. The Radiobiology of Proton Therapy: Challenges and Opportunities Around Relative Biological Effectiveness. *Clinical Oncology* **2018**, *30* (5), 285–292.
- (120) Peeters, A.; Grutters, J. P. C.; Pijs-Johannesma, M.; Reimoser, S.; De Ruysscher, D.; Severens, J. L.; Joore, M. A.; Lambin, P. How costly is particle therapy? Cost analysis of external beam radiotherapy with carbon-ions, protons and photons. *Radiotherapy and Oncology* **2010**, *95* (1), 45–53.
- (121) Zietman, A. L. Too Big to Fail? The Current Status of Proton Therapy in the USA. *Clinical Oncology* **2018**, *30* (5), 271–273.
- (122) Olsen, D. R.; Bruland, Ø. S.; Frykholm, G.; Norderhaug, I. N. Proton therapy – A systematic review of clinical effectiveness. *Radiotherapy and Oncology* **2007**, *83* (2), 123–132.
- (123) Terasawa, T.; Dvorak, T.; Ip, S.; Raman, G.; Lau, J.; Trikalinos, T. A. Systematic Review: Charged-Particle Radiation Therapy for Cancer. *Ann. Int. Med.* **2009**, *151* (8), 556–565.
- (124) Hamada, N.; Imaoka, T.; Masunaga, S.-i.; Ogata, T.; Okayasu, R.; Takahashi, A.; Kato, T. A.; Kobayashi, Y.; Ohnishi, T.; Ono, K.; Shimada, Y.; Teshima, T. Recent Advances in the Biology of Heavy-Ion Cancer Therapy. *Journal of Radiation Research* **2010**, *51* (4), 365–383.
- (125) Okada, T.; Kamada, T.; Tsuji, H.; Mizoe, J. -e.; Baba, M.; Kato, S.; Yamada, S.; Sugahara, S.; Yasuda, S.; Yamamoto, N.; Imai, R.; Hasegawa, A.; Imada, H.; Kiyohara, H.; Jingū, K.; Shinoto, M.; Tsujii, H. Carbon Ion Radiotherapy: Clinical Experiences at National Institute of Radiological Science (NIRS). *Journal of Radiation Research* **2010**, *51* (4), 355–364.
- (126) Tsujii, H.; Kamada, T. A Review of Update Clinical Results of Carbon Ion Radiotherapy. *Japanese Journal of Clinical Oncology* **2012**, *42* (8), 670–685.
- (127) Suit, H.; DeLaney, T.; Goldberg, S.; Paganetti, H.; Clasie, B.; Gerweck, L.; Niemierko, A.; Hall, E.; Flanz, J.; Hallman, J.; Trofimov, A. Proton vs carbon ion beams in the definitive radiation treatment of cancer patients. *Radiotherapy and Oncology* **2010**, *95* (1), 3–22.
- (128) Weber, U. P.; Kraft, G. P. Comparison of Carbon Ions Versus Protons. *Cancer Journal* **2009**, *15* (4), 325–32.
- (129) Akhavan-Rezayat, A.; Palmer, R. B. J. A comparative study of two methods for measuring the stopping power of liquids for alpha particles. *Journal of Physics E: Scientific Instruments* **1980**, *13* (8), 877–881.
- (130) Palmer, R. B. J.; Akhavan-Rezayat, A. The stopping power of water, water vapour and aqueous tissue equivalent solution for alpha particles over the energy range 0.5–8 MeV. *J. Phys. D: Appl. Phys.* **1978**, *11* (4), 605–616.
- (131) Haque, A. K. M. M.; Mohammadi, A.; Nikjoo, H. Study of the Stopping Power and Straggling for Alpha Particles and Protons in Organic Solids, Liquids and Gases. *Radiation Protection Dosimetry* **1985**, *13* (1–4), 71–74.
- (132) Shepard, C.; Kanai, Y. Ion-Type Dependence of DNA Electronic Excitation in Water under Proton, α -Particle, and Carbon Ion Irradiation: A First-Principles Simulation Study. *J. Phys. Chem. B* **2023**, *127* (50), 10700–10709.
- (133) Shepard, C.; Kanai, Y. Ion-Type Dependence of DNA Electronic Excitation in Water under Proton, α -Particle, and Carbon Ion Irradiation: A First-Principles Simulation Study. *J. Phys. Chem. B* **2023**, *127*, 10700.
- (134) Perdew, J. P.; Burke, K.; Ernzerhof, M. Generalized Gradient Approximation Made Simple. *Phys. Rev. Lett.* **1996**, *77* (18), 3865–3868.
- (135) Draeger, E. W.; Andrade, X.; Gunnels, J. A.; Bhatele, A.; Schleife, A.; Correa, A. A. Massively parallel first-principles simulation of electron dynamics in materials. *Journal of Parallel and Distributed Computing* **2017**, *106*, 205–214.
- (136) Kononov, A.; Lee, C.-W.; dos Santos, T. P.; Robinson, B.; Yao, Y.; Yao, Y.; Andrade, X.; Baczewski, A. D.; Constantinescu, E.; Correa, A. A.; Kanai, Y.; Modine, N.; Schleife, A. Electron dynamics in extended systems within real-time time-dependent density-functional theory. *MRS Commun.* **2022**, *12* (6), 1002–1014.
- (137) Andrade, X.; Pemmaraju, C. D.; Kartsev, A.; Xiao, J.; Lindenberg, A.; Rajpurohit, S.; Tan, L. Z.; Ogitsu, T.; Correa, A. A. Inq, a Modern GPU-Accelerated Computational Framework for (Time-Dependent) Density Functional Theory. *J. Chem. Theory Comput.* **2021**, *17* (12), 7447–7467.
- (138) Zhou, R.; Kanai, Y. Molecular Control of Floquet Topological Phase in Non-adiabatic Thouless Pumping. *J. Phys. Chem. Lett.* **2023**, *14* (36), 8205–8212.
- (139) Thouless, D. J. Quantization of particle transport. *Phys. Rev. B* **1983**, *27* (10), 6083–6087.
- (140) Resta, R. Macroscopic polarization in crystalline dielectrics: the geometric phase approach. *Rev. Mod. Phys.* **1994**, *66* (3), 899–915.
- (141) Xiao, D.; Chang, M.-C.; Niu, Q. Berry phase effects on electronic properties. *Rev. Mod. Phys.* **2010**, *82* (3), 1959–2007.
- (142) Ma, W.; Zhou, L.; Zhang, Q.; Li, M.; Cheng, C.; Geng, J.; Rong, X.; Shi, F.; Gong, J.; Du, J. Experimental observation of a generalized Thouless pump with a single spin. *Physical review letters* **2018**, *120* (12), 120501.
- (143) Cerjan, A.; Wang, M.; Huang, S.; Chen, K. P.; Rechtsman, M. C. Thouless pumping in disordered photonic systems. *Light Sci. Appl.* **2020**, *9* (1), 1–7.
- (144) Nakajima, S.; Tomita, T.; Taie, S.; Ichinose, T.; Ozawa, H.; Wang, L.; Troyer, M.; Takahashi, Y. Topological Thouless pumping of ultracold fermions. *Nat. Phys.* **2016**, *12*, 296.
- (145) Lohse, M.; Schweizer, C.; Zilberberg, O.; Aidelsburger, M.; Bloch, I. A Thouless quantum pump with ultracold bosonic atoms in an optical superlattice. *Nat. Phys.* **2016**, *12* (4), 350–354.
- (146) Oka, T.; Kitamura, S. Floquet Engineering of Quantum Materials. *Annual Review of Condensed Matter Physics* **2019**, *10* (1), 387–408.
- (147) Rudner, M. S.; Lindner, N. H. Band structure engineering and non-equilibrium dynamics in Floquet topological insulators. *Nature Reviews Physics* **2020**, *2* (5), 229–244.
- (148) Aharonov, Y.; Anandan, J. Phase change during a cyclic quantum evolution. *Phys. Rev. Lett.* **1987**, *58* (16), 1593–1596.

- (149) Resta, R. Quantum-Mechanical Position Operator in Extended Systems. *Phys. Rev. Lett.* **1998**, *80* (9), 1800–1803.
- (150) Nakagawa, M.; Slager, R.-J.; Higashikawa, S.; Oka, T. Wannier representation of Floquet topological states. *Phys. Rev. B* **2020**, *101* (7), No. 075108.
- (151) Vanderbilt, D. *Berry Phases in Electronic Structure Theory: Electric Polarization, Orbital Magnetization and Topological Insulators*; Cambridge University Press: Cambridge, 2018.
- (152) Asbóth, J. N. K.; Oroszlány, L. S.; Pályi, A. S. *A short course on topological insulators band structure and edge states in one and two dimensions*; Springer: Cham; Heidelberg; New York; Dordrecht; London, 2016.
- (153) Boys, S. F. Construction of some molecular orbitals to be approximately invariant for changes from one molecule to another. *Rev. Mod. Phys.* **1960**, *32* (2), 296.
- (154) Edmiston, C.; Ruedenberg, K. Localized atomic and molecular orbitals. *Rev. Mod. Phys.* **1963**, *35* (3), 457.
- (155) Khouri, J. F.; Schoop, L. M. Chemical bonds in topological materials. *Trends in Chemistry* **2021**, *3* (9), 700–715.
- (156) Martín Pendás, A.; Contreras-García, J.; Pinilla, F.; Mella, J. D.; Cardenas, C.; Muñoz, F. A chemical theory of topological insulators. *Chem. Commun.* **2019**, *55* (82), 12281–12287.
- (157) Becke, A. D. Perspective: Fifty years of density-functional theory in chemical physics. *J. Chem. Phys.* **2014**, *140* (18), 18A301.
- (158) Perdew, J. P.; Schmidt, K. Jacob's ladder of density functional approximations for the exchange-correlation energy. *AIP Conf. Proc.* **2001**, *577* (1), 1–20.
- (159) Furche, F. Developing the random phase approximation into a practical post-Kohn–Sham correlation model. *J. Chem. Phys.* **2008**, *129* (11), 114105.
- (160) Yao, Y.; Kanai, Y. Nuclear Quantum Effect and Its Temperature Dependence in Liquid Water from Random Phase Approximation via Artificial Neural Network. *J. Phys. Chem. Lett.* **2021**, *12* (27), 6354–6362.
- (161) Dick, S.; Fernandez-Serra, M. Machine learning accurate exchange and correlation functionals of the electronic density. *Nat. Commun.* **2020**, *11* (1), 3509.
- (162) Nagai, R.; Akashi, R.; Sugino, O. Completing density functional theory by machine learning hidden messages from molecules. *npj Computational Materials* **2020**, *6* (1), 43.
- (163) Nagai, R.; Akashi, R.; Sasaki, S.; Tsuneyuki, S. Neural-network Kohn-Sham exchange-correlation potential and its out-of-training transferability. *J. Chem. Phys.* **2018**, *148* (24), 241737.
- (164) Maitra, N. T.; Burke, K.; Woodward, C. Memory in Time-Dependent Density Functional Theory. *Phys. Rev. Lett.* **2002**, *89* (2), No. 023002.
- (165) Maitra, N. T. Perspective: Fundamental aspects of time-dependent density functional theory. *J. Chem. Phys.* **2016**, *144* (22), 220901.
- (166) Maitra, N. T.; Zhang, F.; Cave, R. J.; Burke, K. Double excitations within time-dependent density functional theory linear response. *J. Chem. Phys.* **2004**, *120* (13), 5932–5937.
- (167) Kümmel, S.; Kronik, L. Orbital-dependent density functionals: Theory and applications. *Rev. Mod. Phys.* **2008**, *80* (1), 3–60.
- (168) Becke, A. D. A new mixing of Hartree–Fock and local density-functional theories. *J. Chem. Phys.* **1993**, *98* (2), 1372–1377.
- (169) Refaelly-Abramson, S.; Sharifzadeh, S.; Jain, M.; Baer, R.; Neaton, J. B.; Kronik, L. Gap renormalization of molecular crystals from density-functional theory. *Phys. Rev. B* **2013**, *88* (8), No. 081204.
- (170) Skone, J. H.; Govoni, M.; Galli, G. Self-consistent hybrid functional for condensed systems. *Phys. Rev. B* **2014**, *89* (19), 195112.
- (171) Zheng, H.; Govoni, M.; Galli, G. Dielectric-dependent hybrid functionals for heterogeneous materials. *Phys. Rev. Mater.* **2019**, *3* (7), No. 073803.
- (172) Wing, D.; Haber, J. B.; Noff, R.; Barker, B.; Egger, D. A.; Ramasubramaniam, A.; Louie, S. G.; Neaton, J. B.; Kronik, L. Comparing time-dependent density functional theory with many-body perturbation theory for semiconductors: Screened range-separated hybrids and the \$GW\$ plus Bethe-Salpeter approach. *Phys. Rev. Mater.* **2019**, *3* (6), No. 064603.
- (173) Wing, D.; Neaton, J. B.; Kronik, L. Time-Dependent Density Functional Theory of Narrow Band Gap Semiconductors Using a Screened Range-Separated Hybrid Functional. *Advanced Theory and Simulations* **2020**, *3* (12), 2000220.
- (174) Schwegler, E.; Challacombe, M. Linear scaling computation of the Hartree–Fock exchange matrix. *J. Chem. Phys.* **1996**, *105* (7), 2726–2734.
- (175) Shang, H.; Li, Z.; Yang, J. Implementation of screened hybrid density functional for periodic systems with numerical atomic orbitals: Basis function fitting and integral screening. *J. Chem. Phys.* **2011**, *135* (3), No. 034110.
- (176) Burant, J. C.; Scuseria, G. E.; Frisch, M. J. A linear scaling method for Hartree–Fock exchange calculations of large molecules. *J. Chem. Phys.* **1996**, *105* (19), 8969–8972.
- (177) Ochsenfeld, C.; White, C. A.; Head-Gordon, M. Linear and sublinear scaling formation of Hartree–Fock-type exchange matrices. *J. Chem. Phys.* **1998**, *109* (5), 1663–1669.
- (178) Ren, X.; Rinke, P.; Blum, V.; Wieferink, J.; Tkatchenko, A.; Sanfilippo, A.; Reuter, K.; Scheffler, M. Resolution-of-identity approach to Hartree–Fock, hybrid density functionals, RPA, MP2 and GW with numeric atom-centered orbital basis functions. *New J. Phys.* **2012**, *14* (5), No. 053020.
- (179) Prodan, E.; Kohn, W. Nearsightedness of electronic matter. *Proc. Natl. Acad. Sci. U. S. A.* **2005**, *102* (33), 11635–11638.
- (180) Wu, X.; Selloni, A.; Car, R. Order-\$N\$ implementation of exact exchange in extended insulating systems. *Phys. Rev. B* **2009**, *79* (8), No. 085102.
- (181) Ko, H.-Y.; Jia, J.; Santra, B.; Wu, X.; Car, R.; DiStasio, R. A., Jr Enabling Large-Scale Condensed-Phase Hybrid Density Functional Theory Based Ab Initio Molecular Dynamics. I. Theory, Algorithm, and Performance. *J. Chem. Theory Comput.* **2020**, *16* (6), 3757–3785.
- (182) Perdew, J. P.; Ernzerhof, M.; Burke, K. Rationale for mixing exact exchange with density functional approximations. *J. Chem. Phys.* **1996**, *105* (22), 9982–9985.
- (183) Sun, J.; Ruzsinszky, A.; Perdew, J. P. Strongly Constrained and Appropriately Normed Semilocal Density Functional. *Phys. Rev. Lett.* **2015**, *115* (3), No. 036402.
- (184) Yao, Y.; Kanai, Y. Plane-wave pseudopotential implementation and performance of SCAN meta-GGA exchange-correlation functional for extended systems. *J. Chem. Phys.* **2017**, *146* (22), 224105.
- (185) Stephens, P. J.; Devlin, F. J.; Chabalowski, C. F.; Frisch, M. J. Ab Initio Calculation of Vibrational Absorption and Circular Dichroism Spectra Using Density Functional Force Fields. *J. Phys. Chem.* **1994**, *98* (45), 11623–11627.
- (186) Reining, L.; Olevano, V.; Rubio, A.; Onida, G. Excitonic Effects in Solids Described by Time-Dependent Density-Functional Theory. *Phys. Rev. Lett.* **2002**, *88* (6), No. 066404.
- (187) Byun, Y.-M.; Sun, J.; Ullrich, C. A. Time-dependent density-functional theory for periodic solids: assessment of excitonic exchange–correlation kernels. *Electronic Structure* **2020**, *2* (2), No. 023002.
- (188) Botti, S.; Sottile, F.; Vast, N.; Olevano, V.; Reining, L.; Weissker, H.-C.; Rubio, A.; Onida, G.; Del Sole, R.; Godby, R. W. Long-range contribution to the exchange-correlation kernel of time-dependent density functional theory. *Phys. Rev. B* **2004**, *69* (15), 155112.
- (189) Hybertsen, M. S.; Louie, S. G. First-Principles Theory of Quasiparticles: Calculation of Band Gaps in Semiconductors and Insulators. *Phys. Rev. Lett.* **1985**, *55* (13), 1418–1421.
- (190) Rohlfing, M.; Louie, S. G. Electron-Hole Excitations in Semiconductors and Insulators. *Phys. Rev. Lett.* **1998**, *81* (11), 2312–2315.
- (191) Onida, G.; Reining, L.; Rubio, A. Electronic excitations: density-functional versus many-body Green's-function approaches. *Rev. Mod. Phys.* **2002**, *74* (2), 601–659.
- (192) Becke, A. D. A new mixing of Hartree–Fock and local density-functional theories. *J. Chem. Phys.* **1993**, *98* (2), 1372–1377.

- (193) Lee, C.; Yang, W.; Parr, R. G. Development of the Colle-Salvetti correlation-energy formula into a functional of the electron density. *Phys. Rev. B* **1988**, *37* (2), 785–789.
- (194) Xu, B.-X.; Rajagopal, A. K. Current-density-functional theory for time-dependent systems. *Phys. Rev. A* **1985**, *31* (4), 2682–2684.
- (195) Vignale, G.; Kohn, W. Current-Dependent Exchange-Correlation Potential for Dynamical Linear Response Theory. *Phys. Rev. Lett.* **1996**, *77* (10), 2037–2040.
- (196) Maitra, N. T.; Souza, I.; Burke, K. Current-density functional theory of the response of solids. *Phys. Rev. B* **2003**, *68* (4), No. 045109.
- (197) Vignale, G.; Ullrich, C. A.; Conti, S. Time-Dependent Density Functional Theory Beyond the Adiabatic Local Density Approximation. *Phys. Rev. Lett.* **1997**, *79* (24), 4878–4881.
- (198) Wijewardane, H. O.; Ullrich, C. A. Time-Dependent Kohn-Sham Theory with Memory. *Phys. Rev. Lett.* **2005**, *95* (8), No. 086401.
- (199) Ullrich, C. A. Time-dependent density-functional theory beyond the adiabatic approximation: Insights from a two-electron model system. *J. Chem. Phys.* **2006**, *125* (23), 234108.
- (200) Yonehara, T.; Hanasaki, K.; Takatsuka, K. Fundamental Approaches to Nonadiabaticity: Toward a Chemical Theory beyond the Born–Oppenheimer Paradigm. *Chem. Rev.* **2012**, *112* (1), 499–542.
- (201) Li, X.; Tully, J. C.; Schlegel, H. B.; Frisch, M. J. Ab initio Ehrenfest dynamics. *J. Chem. Phys.* **2005**, *123* (8), No. 084106.
- (202) Horsfield, A. P.; Bowler, D. R.; Fisher, A. J.; Todorov, T. N.; Montgomery, M. J. Power dissipation in nanoscale conductors: classical, semi-classical and quantum dynamics. *J. Phys.: Condens. Matter* **2004**, *16* (21), 3609.
- (203) Capitani, J. F.; Nalewajski, R. F.; Parr, R. G. Non-Born–Oppenheimer density functional theory of molecular systems. *J. Chem. Phys.* **1982**, *76* (1), 568–573.
- (204) Gidopoulos, N. Kohn-Sham equations for multicomponent systems: The exchange and correlation energy functional. *Phys. Rev. B* **1998**, *57* (4), 2146–2152.
- (205) Kreibich, T.; Gross, E. K. U. Multicomponent Density-Functional Theory for Electrons and Nuclei. *Phys. Rev. Lett.* **2001**, *86* (14), 2984–2987.
- (206) Pavošević, F.; Culpitt, T.; Hammes-Schiffer, S. Multi-component Quantum Chemistry: Integrating Electronic and Nuclear Quantum Effects via the Nuclear–Electronic Orbital Method. *Chem. Rev.* **2020**, *120* (9), 4222–4253.
- (207) Hammes-Schiffer, S. Nuclear–electronic orbital methods: Foundations and prospects. *J. Chem. Phys.* **2021**, *155* (3), No. 030901.
- (208) Colle, R.; Salvetti, O. Approximate calculation of the correlation energy for the closed shells. *Theoretica chimica acta* **1975**, *37* (4), 329–334.
- (209) Yang, Y.; Brorsen, K. R.; Culpitt, T.; Pak, M. V.; Hammes-Schiffer, S. Development of a practical multicomponent density functional for electron-proton correlation to produce accurate proton densities. *J. Chem. Phys.* **2017**, *147* (11), 114113.
- (210) Zhao, L.; Tao, Z.; Pavošević, F.; Wildman, A.; Hammes-Schiffer, S.; Li, X. Real-Time Time-Dependent Nuclear–Electronic Orbital Approach: Dynamics beyond the Born–Oppenheimer Approximation. *J. Phys. Chem. Lett.* **2020**, *11* (10), 4052–4058.
- (211) Xu, J.; Zhou, R.; Tao, Z.; Malbon, C.; Blum, V.; Hammes-Schiffer, S.; Kanai, Y. Nuclear–electronic orbital approach to quantization of protons in periodic electronic structure calculations. *J. Chem. Phys.* **2022**, *156* (22), 224111.
- (212) Dempsey, J. L.; Heyer, C. M.; Meyer, G. J. A Vision for Sustainable Energy: The Center for Hybrid Approaches in Solar Energy to Liquid Fuels (CHASE). *Electrochemical Society Interface* **2021**, *30* (1), 65.
- (213) Zhao, R.; You, P.; Meng, S. Ring Polymer Molecular Dynamics with Electronic Transitions. *Phys. Rev. Lett.* **2023**, *130* (16), 166401.
- (214) Craig, I. R.; Manolopoulos, D. E. Quantum statistics and classical mechanics: Real time correlation functions from ring polymer molecular dynamics. *J. Chem. Phys.* **2004**, *121* (8), 3368–3373.
- (215) Habershon, S.; Manolopoulos, D. E.; Markland, T. E.; Miller, T. F. Ring-Polymer Molecular Dynamics: Quantum Effects in Chemical Dynamics from Classical Trajectories in an Extended Phase Space. *Annu. Rev. Phys. Chem.* **2013**, *64* (1), 387–413.
- (216) Ananth, N. Path Integrals for Nonadiabatic Dynamics: Multistate Ring Polymer Molecular Dynamics. *Annu. Rev. Phys. Chem.* **2022**, *73* (1), 299–322.
- (217) Abedi, A.; Maitra, N. T.; Gross, E. K. U. Exact Factorization of the Time-Dependent Electron-Nuclear Wave Function. *Phys. Rev. Lett.* **2010**, *105* (12), 123002.
- (218) Requist, R.; Gross, E. K. U. Exact Factorization-Based Density Functional Theory of Electrons and Nuclei. *Phys. Rev. Lett.* **2016**, *117* (19), 193001.
- (219) Agostini, F.; Gross, E. K. U. Ultrafast dynamics with the exact factorization. *European Physical Journal B* **2021**, *94* (9), 179.
- (220) Talotta, F.; Agostini, F.; Ciccotti, G. Quantum Trajectories for the Dynamics in the Exact Factorization Framework: A Proof-of-Principle Test. *J. Phys. Chem. A* **2020**, *124* (34), 6764–6777.
- (221) Li, T. E.; Tao, Z.; Hammes-Schiffer, S. Semiclassical Real-Time Nuclear-Electronic Orbital Dynamics for Molecular Polaritons: Unified Theory of Electronic and Vibrational Strong Couplings. *J. Chem. Theory Comput.* **2022**, *18* (5), 2774–2784.
- (222) Flick, J.; Ruggenthaler, M.; Appel, H.; Rubio, A. Atoms and molecules in cavities, from weak to strong coupling in quantum-electrodynamics (QED) chemistry. *Proc. Natl. Acad. Sci. U. S. A.* **2017**, *114* (12), 3026–3034.
- (223) Sato, S. A.; Yabana, K. Maxwell + TDDFT multi-scale simulation for laser-matter interactions. *Journal of Advanced Simulation in Science and Engineering* **2014**, *1* (1), 98–110.
- (224) Tully, J. C. Molecular dynamics with electronic transitions. *J. Chem. Phys.* **1990**, *93* (2), 1061–1071.
- (225) Craig, C. F.; Duncan, W. R.; Prezhdo, O. V. Trajectory Surface Hopping in the Time-Dependent Kohn-Sham Approach for Electron-Nuclear Dynamics. *Phys. Rev. Lett.* **2005**, *95* (16), 163001.
- (226) Wang, L.; Akimov, A.; Prezhdo, O. V. Recent Progress in Surface Hopping: 2011–2015. *J. Phys. Chem. Lett.* **2016**, *7* (11), 2100–2112.
- (227) Secor, M.; Soudackov, A. V.; Hammes-Schiffer, S. Artificial Neural Networks as Propagators in Quantum Dynamics. *J. Phys. Chem. Lett.* **2021**, *12* (43), 10654–10662.
- (228) Lin, K.; Peng, J.; Xu, C.; Gu, F. L.; Lan, Z. Automatic Evolution of Machine-Learning-Based Quantum Dynamics with Uncertainty Analysis. *J. Chem. Theory Comput.* **2022**, *18* (10), 5837–5855.
- (229) Prezhdo, O. V.; Rossky, P. J. Relationship between Quantum Decoherence Times and Solvation Dynamics in Condensed Phase Chemical Systems. *Phys. Rev. Lett.* **1998**, *81* (24), 5294–5297.
- (230) Simonius, M. Spontaneous Symmetry Breaking and Blocking of Metastable States. *Phys. Rev. Lett.* **1978**, *40* (15), 980–983.
- (231) Kilina, S. V.; Neukirch, A. J.; Habenicht, B. F.; Kilin, D. S.; Prezhdo, O. V. Quantum Zeno Effect Rationalizes the Phonon Bottleneck in Semiconductor Quantum Dots. *Phys. Rev. Lett.* **2013**, *110* (18), 180404.
- (232) Jaeger, H. M.; Fischer, S.; Prezhdo, O. V. Decoherence-induced surface hopping. *J. Chem. Phys.* **2012**, *137* (22), 22A545.
- (233) Wong, J. C.; Kanai, Y. Quantum Confinement and Decoherence Effect on Excited Electron Transfer at the Semiconductor–Molecule Interface: A First-Principles Dynamics Study. *J. Phys. Chem. C* **2023**, *127* (1), 532–541.
- (234) Di Ventra, M.; D’Agosta, R. Stochastic Time-Dependent Current-Density-Functional Theory. *Phys. Rev. Lett.* **2007**, *98* (22), 226403.
- (235) Appel, H.; Ventra, M. D. Stochastic quantum molecular dynamics for finite and extended systems. *Chem. Phys.* **2011**, *391* (1), 27–36.

- (236) Prezhdo, O. V. Mean field approximation for the stochastic Schrödinger equation. *J. Chem. Phys.* **1999**, *111* (18), 8366–8377.